Lifespan associated changes in global patterns of coherent communication

Bikash Sahoo[1]; Anagh Pathak[1**]; Gustavo Deco[2], Arpan Banerjee[1*]; Dipanjan Roy[1*]**

[1] Cognitive Brain Dynamics Lab National Brain Research Centre (NBRC), NH8 Nainwal Mode 122051 Manesar, Haryana, India

[2] Institució Catalana de la Recerc Estudis Avançats (ICREA), Universitat Pompeu Fabra, Passeig Lluís, Companys 23, Barcelona, 08010, Spain

** Equal contributions

***corresponding authors**

dipanjan.nbrc@gov.in; arpan@nbrc.ac.in

Keywords: Healthy Ageing, Peak Alpha, Global coherence, Metastability, Multifrequency

Abstract

Cognitive processes are mediated by communication among multiple brain areas using frequency specific interactions. These frequency specific interactions are fundamental for attention, perception, learning and memory as highlighted by extant literature. Individually, brain

areas exhibit oscillatory neuro-electromagnetic signals emerging from a cascade of complex physiological processes. Efficient cognition demands seamless interaction between these different oscillatory modules of the brain. Recent models of large scale spontaneous brain activity have underscored the importance of brain-wide coherence in bringing about facilitative patterns of activity. Additionally, the allied but independent concept of global metastability casts the understanding of the transient nature of stability of brain connectivity patterns within a dynamic framework.

Since healthy ageing is accompanied by changes in large-scale spontaneous electromagnetic oscillations, we asked if the variability and complexity of communication between brain areas with aging could be quantified with global coherence and metastability. Finding such patterns in resting state MEG would naturally pave the way for tracking task relevant changes in metastability and coherence dynamics that could crucially determine cognitive flexibility and performance in elderly individuals. While previously reported observations of a reduction in peak alpha frequency and increased beta power in older adults are reflective of changes at individual sensors (during rest and task), global coherence and metastability truly pinpoint the underlying coordination dynamic across multiple brain areas across the entire lifespan. This study was not only able to replicate the previous observations in a substantially larger lifespan cohort than what was previously reported, we also demonstrate, for the first time to the best of our knowledge, age related changes in coherence and metastability. Furthermore, we observed a marked frequency dependence in changes in global coordination dynamics, which, coupled with the long held view of specific frequency bands sub serving different aspects of cognition, hints at different functional processing roles for slower and faster brain dynamics.

Introduction:

A comprehensive understanding and characterization of the process of healthy aging is essential to treat age-associated neurological changes such as decline in working memory, processing speeds and executive cognitive functioning. Over the years, converging lines of evidence have successfully demonstrated the role of neural oscillations in many of the above mentioned cognitive faculties. Specific neuronal oscillatory patterns observed in EEG/ MEG data are essential markers of cognition (Buzsaki 2011), and researchers overwhelmingly agree on the use of field potential to tap neuro-cognitive processes associated with human brain

function (Pesaran et al., 2018). Accordingly, a number of recent studies have tried to track age-related changes in the brain's oscillatory profile using spectral estimation techniques. For example, the amplitude of resting and motor related beta band oscillations (16-25 Hz) is typically found to be higher in the older population compared to the younger population. Similarly, substantial number of reports have highlighted that spontaneous peak alpha frequency (8-12 Hz) is lower in older as compared to younger participants.

While age-related alterations in sensor specific features like power and frequency are fairly well reported, very few studies have looked at changes in global patterns of frequency specific synchronization in the context of healthy ageing. We argue that much information about the mechanisms of ageing is to be found in studying patterns of coherent activity across lifespan. The relevance of this assumption can be assessed from extant literature. For example, the theory of communication through coherence (CTC) posits that message passing across spatially distant neural assemblies demands coordinated fluctuations in their respective excitabilities(Fries, 2005). The importance of global coherence in the context of cognitive functioning is underscored by the essential need for efficient message passing in bringing about cognition. Even though the original CTC proposal was formulated in a task context, recent work has drawn out its repercussions for spontaneous brain dynamics, a.k.a resting state activity(Deco et.al.,2016). According to this formulation, resting brain activity constantly traverses across different functional configurations in order to maintain a state of maximal readiness in anticipation of external stimuli, which, when presented, collapses the state of the brain to whichever configuration is deemed most relevant in the stimulus context. In other words, resting state brain activity must demonstrate metastable dynamics, whereby the brain fluidly recapitulates varied patterns of coherent activity(Deco et.al.,2016). In line with this view, global metastability is found to be associated with cognitive flexibility and information processing in the brain. Therefore, tracking changes in coherence and metastability is crucial, given the fact that ageing is marked by distinct cognitive changes that are, in turn, orchestrated by coherent neural oscillations.

The fundamental objective of this article is to track lifespan changes in patterns of global coherence and metastability by using appropriate measures that can tease out these metrics from neurophysiological recordings. As a necessary confirmatory step, we first replicate the already well-established results in the field of ageing neuroscience- the observations of reduced peak alpha frequency and an increase in average beta power with age on the current dataset. In

doing so, we successfully establish the validity of earlier observations on a substantially larger dataset across the age continuum - a feature lacking in many earlier studies. We then utilize a standard measure of global coherence to characterize band specific lifespan trends. Finally, we apply a proxy for metastability- the standard deviation of the Kuramoto order parameter, to characterize age-related alterations in frequency specific metastable brain dynamics.

We employ the resting-state magnetoencephalogram (MEG) recordings from the Cambridge-Ageing Neuroscience (Cam-CAN) group for our purposes. Since this analysis has been carried out on a large cohort of an aging population (cross-sectional) consisting of 650 participants across an age range of 18-88 years, the findings can be considered to be highly robust and reliable.

We provide empirical evidence for lifespan changes in global patterns of coherence on the sensor level. Notably, we observe the emergence of a temporal dichotomy between slower and faster oscillations in the way they evolve with age, suggestive of different processing roles.

Methods

Subject details

Cam-CAN is a multi-modal, cross-sectional adult life-span population-based study. The study was approved by the Cambridgeshire 2 Research Ethics Committee, and all participants have given written informed consent. The data presented here belonged to Stage 2 of the study. In Stage-1, 2681 participants had been home-interviewed and had gone through neuropsychological assessments and been tested for vision, balance, hearing and speeded response. Participants with poor vision (< 20/50 on Snellen test), poor hearing (threshold greater than 35 dB at 1000 Hz in both ears), past history of drug abuse, with any psychiatric illness such as bipolar disorder, schizophrenia, with neurological disease e.g. epilepsy, stroke, traumatic brain injury, or a score less than 25 in Mini-Mental State Examination were excluded from further behavioral and neuroimaging experiments. 700 participants had been screened from Stage 1 to Stage 2, of which Magnetoencephalogram(MEG) data from 650 subjects were available.

Data acquisition

Data used in the preparation of this work were obtained from the CamCAN repository (available at http://www.mrc-cbu.cam.ac.uk/datasets/camcan/) (Taylor et al., 2016, Shafto et al., 2015). For all the subjects, MEG data were collected using a 306-sensor (102 magnetometers and 204 orthogonal planar magnetometers) VectorView MEG System by Elekta Neuromag, Helsinki, located at MRC-CBSU. Data were digitized at 1 kHz with a high pass filter of cutoff 0.03 Hz. Head position was monitored continuously using four Head Position Indicator coils. Horizontal and vertical electrooculogram were recorded using two pairs of bipolar electrodes. One pair of bipolar electrodes were used to record electrocardiogram for pulse-related artifact removal during offline analysis.

The data presented here consisted only of resting state, where the subject sat still with their eyes closed for a minimum duration of 8 minutes and 40 seconds.

Data preprocessing

Preprocessed data was provided by Cam-CAN research consortium, where for each run temporal signal space separation was applied to remove noise from the environment, from Head Position Indicator coils, line noise and for the detection and reconstruction of the signal from noisy sensors. All the data had been transformed into a common head-position. More details about data acquisition and preprocessing have been presented elsewhere (Taylor et al., 2017; Shafto et al., 2014).

Data analysis

Welch spectrum

Fieldtrip toolbox(Oostenveld et al.,2011) was used to read the data provided in ‘.fif’ format. For each individual, data was downsampled from 1 kHz to 250 Hz. First, we sought to investigate age specific changes in the spectral densities of the raw MEG signals.

Time series corresponding to the 102 magnetometers, resulted in a matrix X of size $102 \times T$, where T corresponds to number of time points. Power spectral density for each sensor c's time series $x_c(t)$ was estimated using Welch's periodogram method. Each time series was divided into segments of 20 seconds without any overlap between segments. Spectrum was estimated for each segment after multiplying it with a Hanning window. Spectrums of all the segments were finally averaged.

We estimated a global spectrum, representative of each subject i.e. $S_I(f)$ by taking a grand average across the spectrums belonging to all magnetometers.

$$S_I(f) = \sum_c s_I(c, f) \qquad (1)$$

Quantification of spatial overlap between sources of alpha and beta activity in the sensor space

For each subject, the sensor map of alpha and beta activity were normalized separately.

$$\hat{\alpha}_I(c) = \frac{\alpha_I(c) - \langle \alpha_I \rangle}{\sigma_{\alpha(I)}} \qquad (2)$$

$$\hat{\beta}_I(c) = \frac{\beta_I(c) - \langle \beta_I \rangle}{\sigma_{\beta(I)}} \qquad (3)$$

where $\sigma_{\alpha(I)}$ and $\sigma_{\beta(I)}$ are the standard deviations of alpha and beta band respectively. Separation between the normalized sensor level representation $\hat{\alpha}_I$ and $\hat{\beta}_I$ was indexed by the cosine angle between the two multidimensional vectors.

$$\hat{\theta}(\alpha, \beta) = \cos^{-1}\left(\frac{\hat{\alpha}_I . \hat{\beta}_I}{|\hat{\alpha}_I| |\hat{\beta}_I|} \right) \qquad (4)$$

The angular separations across age were statistically analyzed using Spearman rank correlations and t-tests.

Global coherence

To measure the covariation of neural oscillations on a global level, we employed a technique known as global coherence (Cimenser et al., 2008;Kumar et al.,2016). Global coherence among sensors at any frequency f is measured as the percentage of variance explained by the first eigenvector of the cross spectral density matrix at f .

In an individual subject's data, for each sensor, the time series $x(t)$ was divided into N non-overlapping windows of 5 seconds duration each i.e. $y(t)$. This resulted an average of 112 (median, Interquartile range 1, range 70-220) windows for each subject. We considered 3 orthogonal discrete prolate spheroidal sequences, also known as Slepian tapers, to avoid leakage in spectral estimates into nearby frequency bands. The time-bandwidth product was taken to be 2, which resulted in a bandwidth of 0.4 Hz.

Before computing FFT, each data segment was detrended i.e. from each data segment $y(t)$ the best straight line fit was regressed out.

$$\hat{y}(t) = y(t) - \underline{y}(t) \quad (5)$$

where $\underline{y}(t)$ is the straight line fit of $y(t)$. Each segment was multiplied with a set of 3 orthogonal Slepian tapers and fast fourier transform was applied to the tapered segments.

Computing the complex FFT(for T tapers) at frequency f for each segment n of sensor c resulted in a complex matrix Y of dimension $F \times C \times N \times T$. We utilized the chronux(Bokil et al., 2010) library to perform the global coherence analysis.

Cross spectral density between two sensors was estimated from $\hat{Y}$ by using the formula

$$S_f(i,j) = \frac{1}{N} \sum_n \sum_T conj\left(\hat{Y}(f,i,n,T)\right) \times \hat{Y}(f,j,n,T) \quad (6)$$

where i and j are the channel indices, f is the frequency index n is the segment index and T is the taper.

Singular value decomposition was applied to the cross spectral density matrix S_f for each frequency value f .

$$S_f = US\,U^T \quad (7)$$

Diagonals of S would be proportional to the explained variance by the orthogonal set of eigenvectors U . The values of S were normalized so that each entry denote the percentage of the net variance explained in S_f .

$$\hat{S} = \frac{S}{\sum_i S(i)} \quad (8)$$

The first entry of $\hat{S}$ is defined as the global coherence. Global coherence was computed for each frequency value f, resulting an array G of length F.

Metastability

We calculated the metastability measure for all participants across all magnetometer sensors. Metastability is defined as variability of the Kuramoto Order parameter, $R(t)$, which is given as,

$$R(t)e^{i\psi(t)} = \frac{1}{N}\sum_N e^{i\phi_n(t)} \quad (9)$$

Where φ_n is the phase of the nth oscillator and ψ is the mean phase of the system of oscillators. In this analysis, every MEG sensor is conceptualized as a coupled oscillator, summarized by its instantaneous phase $\phi(t)$. At any given point of time, the phase of each oscillator is extracted and projected onto a polar coordinate system, as a unit vector($e^{i\phi_n(t)}$). The length of the resultant vector, obtained from averaging all the unit vectors is interpreted as the Kuramoto Order parameter, $R(t)$. The temporal variability of R, as measured by the standard deviation, is taken to be the metastability(Deco et.al.,2017).

As a first step, the pre-processed resting state time series was band-pass filtered so as to obtain filtered time series. Instantaneous phase of each filtered band was estimated from the filtered data for metastability calculation. The pass band for the band-pass filtering step was kept narrow so that the resulting phase is readily interpretable.

For this analysis, each time series was filtered in the following 8 bands- 2-4 Hz, 3-7 Hz, 8-12 Hz, 12-16 Hz, 16-20 Hz, 20-24 Hz, 24-28 Hz and 28-32 Hz. As mentioned earlier, the choice of frequency bands was dictated by phase considerations. An additional criteria was to chunk the frequency bands so that they map onto well-known frequency bands such as delta, theta, alpha and beta. The beta band was further split into 5 smaller, non-overlapping bands. As mentioned earlier, we restricted our analysis to below 40 Hz due to presence of HPI noise.

FieldTrip toolbox(ft_preproc_bandpassfilter.m) was used to band-pass filter each signal in the appropriate frequency bands. This routine was used to implement a finite impulse response(FIR), two-pass filter that preserves phase information of the time series.

Subsequently, instantaneous phase was estimated by using built-in MATLAB implementation of the hilbert transform(hilbert.m). The resulting phase time series for each channel and participant was used to calculate band and subject specific metastability.

Similar to the preceding analysis, metastability analysis was performed by 1.)treating age as a continuous variable 2.) binning participants in the following age brackets - 18-35 yr(Young Adults), 36-50 yr(Middle Age), 51-65 yr(Middle Elderly) and 66 -88 yr (Elderly).

For the region-wise analysis, the brain was segmented into 5 non-overlapping regions(frontal, centro-parietal, occipital, left and right temporal). Metastability index was calculated individually for all regions separately by randomly sampling 14 sensors from each region. Metastability was tracked as a function of age by calculating the Spearman rank correlations.

Results

For majority of analysis carried out in this work, we have considered age to be a continuous variable. However, for certain analysis we have divided the age values of total N=650 subjects into four age groups (Young Adults (YA), Middle Elderly (ME), Middle Late (ML), Older Adults (OA)), for which the demographic information has been provided in **table 1**.

Age group	N	% Female
YA (18-35)	126	55
ME (36-50)	159	49
ML (51-65)	149	50
OA (66-88)	216	46

Table1. Sample size and gender in each representative age group

Spectral properties of neural oscillations with aging

We started with spectral estimation of the resting state data to investigate the effect of healthy ageing on the fundamental properties of the endogenous band-limited neural oscillations such as amplitude and center frequency. Since the Head Position Indicator(HPI) coil related noise can be unreliable at higher frequencies we concentrated our analysis between 0-40Hz which fully contains the neural oscillations in the Delta(<4Hz), Theta(4-8Hz), Alpha(8-12Hz), and Beta(16-25Hz) frequency bands.

Figure 1A shows the average global spectrum of four different age groups. Qualitative changes can be seen in the spectrum among age groups in both Alpha and Beta oscillations. A gradual increase in Beta band power was seen with increase in age and a shift in the peak Alpha frequency (PAF) was observed between the youngest and oldest age group. Motivated by these qualitative results we further sought to quantify the statistical significance of ageing related difference and possible neural implications of these changes in the spectrum of Alpha and Beta band oscillations.

Alpha band power was estimated by averaging the estimated spectral values within 8-12 Hz. Estimated Alpha band powers were grouped according to the four age groups. Since the number of subjects within each age group were not uniform, for further statistical comparison between two groups we always chose the minimum number of subjects among the age groups i.e. 126 for the YA group. We randomly sampled 126 values from each group and performed unpaired t-test. The sampling was iterated over 5000 times. Correction was made for multiple comparison using False Discovery Rate procedure (Benjamini and Hochberg, 1995). Using Kruskal-Wallis test, we did not find any significant difference in alpha power among age groups ($p = 0.991$). Performing t-test among any two groups for alpha power didn’t show any significance either.

Beta band power was estimated by averaging the estimated spectral values within 16-25 Hz.

Beta powers were grouped into four age groups and similar statistics were performed as explained in the previous subsection. **Figure 1B** shows variation in beta power among four age groups. We found significant effect of age on beta band activity (R^2=0.04, P<0.001, N=650). Significant differences were seen between age groups YA, 18-35 years and ME, 36-50 years (t(250) = -3.55, p = 0.001), groups YA and ML, 51-65 years (t(250) = -4.51, p < 0.001), groups YA and OA, 66-88 years (t(250) = -5.60, p < 0.001) and a marginally significant difference was observed between groups ME and OA (t(250) = -2.05, p = 0.070). Spearman's rank correlation between age of the individual and beta power was found to be 0.216, p < 0.001, which suggests beta activity increases with aging.

Peak Frequency shift for alpha band: Spatiotemporal Organization

Frequency value at which there was maximum activity in the alpha band i.e. 8-12 Hz for a subject, was taken to be the peak alpha frequency of that subject. **Figure 1C** is an age-spectrogram which shows variation in the power spectral density in the alpha band with age. Age values were grouped into bins of 5 years starting from 18 years. The bins were non-overlapping and the center of each bin was considered as the representative age value of the bin. We found significant effect of age on center alpha frequency (R^2=0.14, P<0.001, N=650). Spearman's rank correlation between age and center frequency in the alpha band was found to be -0.384 (p < 0.001).

Further we investigated the variation of peak alpha frequency with aging at individual sensor level. **Figure 1D** shows the topographical map of Spearman's rank correlation between peak alpha frequency and age. Overall, peak alpha frequency decreased with age in many sensors and had a statistically significant negative correlation with age. Surprisingly, a set of sensors in the prefrontal cortex did not show a robust decrease in peak alpha frequency with age. In these sensors, either the correlation was low or nonsignificant(sensor groups indicated in yellow, innermost contour,**Fig 1D**,average Spearman's rank correlation, -0.0248, p=0.5284).

Whole brain measures of neuronal communication states during ageing

Presence of large-scale functional brain networks was investigated using global coherence across all MEG sensors at different frequencies for each subject(Cimenser et al,2011; Kumar et

al. 2016). **Figure 2** shows the average of the global coherence spectrum for the four age groups. Qualitative differences were observed across frequency range 0-25 Hz, which were quantified and tested for statistical significance.

Global coherence at all the frequency values within a frequency band were averaged to generate a representative value for the corresponding frequency band in four age groups, YA, ME, ML, OA (Fig 1A) . In order to track lifespan trajectories, subjects were grouped into finer non-overlapping age bins of 5 years between 18-88 years. Representative global coherence in age bin was averaged and standard error was computed for each age bin (Fig 2B).

2-way ANOVA test revealed an age effect F(1,3) = 4.74,p = 0.0027, a frequency effect of F(1,3) = 174.79, p < 0.001 and an interaction effect of F(1,9) = 9.23, p <0.001. We observed that the global coherence in Delta band, 1-3 Hz ($y=0.0006x+0.2863, R^2=0.077, p<0.001, N=650$), in Theta band, 3-7 Hz ($y=0.0004x+0.2583, R^2=0.063, p<0.001, N=650$), and Alpha band, 8-12 Hz $\left(y=0.0013x+0.4168, R^2=0.076, p<0.001, N=650\right)$ was correlated with age. Correlation of age with global coherence in Beta band (16-25 Hz) was small ($y=-0.0002x+0.2584$, $R^2=0.021, p<0.001$, $N=650$). Thus we suspected that age had a differential effect vis-a-vis global coherence depending on the time scale of the oscillations. To test our hypothesis that age related reorganization results in differential processing in slower and faster time scales we have further divided the oscillations into two major groups i.e. of slow time scale (1-5 Hz) and of fast timescale (10-20 Hz). As expected from the previous set of results we found significant increase in global coherence with increase in age for slow oscillations (Spearman's rank correlation $c=0.248, p<0.001$) and a significant decrease with aging in fast oscillations (Spearman's rank correlation $c=-0.356, p<0.001$).

Topographical segregation of neural oscillations at different time-scales with aging

Next, we investigated the spatial boundaries of whole brain networks corresponding to age-related difference along slow and fast time scales of neuronal signal using subspace analysis borrowed from linear algebra. The key findings confirm our hypothesis that the topographical changes of the spectral power with aging i.e. the changes on the scalp level representation of

Alpha and Beta band activity increases with age. Here, for simplicity, we considered only the two extreme age groups i.e. YA (18-35) and OA (66-88). **Figure 3A** shows the average topographical map of alpha activity at the center alpha frequency and average beta activity in 16-25 Hz for the youngest and oldest age groups. Performing cluster based permutation statistics revealed statistically significant patterns of difference in alpha and beta band activity between the two age groups.

Although, we observed similar patterns of difference between the oldest and youngest age groups for global alpha band power and beta band power, there seemed to be a qualitative difference in the overlap of sensors representing alpha activity and beta band activity. We quantified the overlap between these two sensor topographies by the angle between their respective vector representations. Larger angles indicated more separation and less topological overlap between sensor groups.

We found significant effect of age on the angle between Alpha and Beta band activities' sensor wise representation ($R^2=0.056, p<0.001, N=650$). **Fig 3C** shows how angular separation of subspaces between scalp topographies from underlying alpha and beta frequencies increase as a function of age. Significant difference was found between age groups 18-34 and 51-65 (t(228) = -2.89, p = 0.011), age groups 18-34 and 66-88 (t(228) = -4.64, p < 0.001) and age groups 35-50 and 66-88 (t(228) = -3.42, p = 0.003).

Metastability and aging

We estimated the variability of neuronal communication states using metastability as a function of age and frequency. We observed a dichotomous pattern in metastability as a function of frequencies in all age groups, a sharp decrease with increasing frequencies till 12 Hz and a gradual increase in the metastability indices across frequencies between 12-40Hz(Fig 4) . This was further confirmed by treating age as a continuous parameter and also by chunking participants in 4 age-groups as highlighted in previous subsections.

To identify the statistical trends we grouped the participants in 4 age groups and performed t-test across the age-groups. Statistics similar to the power analysis was performed to confirm the

correlation of age and metastability. A 2-way ANOVA test revealed a age effect $F(1,3) = 64.41, p \sim 0$, a frequency effect of $F(1,7) = 35.61$, $p \sim 0$ and a interaction effect of $F(1,21) = 2.08$, $p = 0.0027$. Subjects were divided in four age groups and unpaired t-tests were performed by drawing 5000 samples from each age group. Every random draw consisted of subjects equal to the smallest age group (126, Young). Resulting p-values were corrected for multiple comparisons by using the procedure described in (Benjamini-Hochberg,1995) and implemented using MATLAB functions. The following p-values and t-statistics were obtained for metastability in alpha band- YA vs ME ($p=0.07,\ t = -1.97$), YA vs ML($p<0.001$, $t= -4.52$), YA vs E($p<0.001, t=-4.332$), ME vs ML($p= 0.0220,\ t= -2.5646$), ME vs E($p=0.0284, t=-2.445$), ML vs E($p=0.7542,\ t= -0.1703$).

Differential profiles of slow vs. fast scales of metastability in aging

Our findings suggest a characteristic U-shaped profile of metastability as a function of various frequency bands. Interestingly, the minimum metastability was observed in the alpha frequency band, consistent across age groups (see Fig. 4). The comparison of metastability in slow and fast time scales across age-groups revealed an interesting inverse trend. The metastability associated with slower time scales (Delta and Theta) was found to be lower than the corresponding values for the faster time scales (Beta 4,5) in the young cohort ($p<0.001$) whereas the opposite trend was observed in the elderly group ($p=0.0075$)). This was further confirmed by pooling the metastability values of the slower and faster time scales together and performing non-parametric statistical tests (two sample Kolmogorov-Smirnov test (KS-test)).

Region Wise analysis of metastability reveals differential trends

In order to track changes in metastability in specific brain areas we segmented the sensors in 5 groups - Frontal, Centro-Parietal, Occipital, Left Temporal and Right Temporal regions. The region-wise analysis consisted of 14 randomly sampled sensors in each brain region. Next, we calculated region-wise metastability and tracked its change with aging. Spearman rank correlation was performed to characterize trends in band and region specific metastability.

This suggests that whereas Alpha band displays an increasing trend with age for all brain regions, Delta and Theta oscillations either stayed invariant or reduced as a function of age in the occipital, left temporal and right temporal regions. Beta band metastability showed the highest age correlation(using Spearman rank test) in the centro-parietal sensors while staying invariant in the occipital and temporal sensors.

The following Spearman rank coefficients were obtained for delta band - frontal (*c=0.2499, p<0.001*), centro-parietal *(c=0.1629, p<0.001*), occipital (*c=-0.0686, p=0.0805*), left temporal (*c~0,p=0.92*), right temporal (*c=-0.1428, p<0.001*). The corresponding values for alpha band were frontal (c=0.2161, p<0.001), centro-parietal (*c=0.1808,p<0.001*), occipital (*c=0.1348, p<0.001*), left temporal (*c=0.2030, pval<0.001*), right temporal (*c=0.2070, p<0.001*). For theta band- frontal (*c=0.1725, p<0.001*), centro-parietal (*c=0.2049, pval<0.001*), occipital (*c=-0.1141, pval=0.0036*), left-temporal(*c=-0.04, p=0.2396*), right-temporal(*c=-0.0457, p=0.2443*) were obtained. We tracked metastability in the beta band for three frequency bands ($\beta_1, \beta_3, \beta_5$) using similar statistical methodology. Centro-parietal sensors showed the highest age related positive correlations (c=0.2046, 0.2542, c=0.1734, p<0.001 for the three bands respectively).

Relationship of global coherence with cognition

Recent reports have suggested a relationship between alpha band activity and short term memory. We also find a significant correlation between global coherence in the alpha band and precision in a visual short term memory task(Zhang et. al., 2008) after regressing out the effect of age(Figure 6). Significance was tested by performing partial correlations(matlab partialcorr.m), considering age as a covariate;rho = 0.09, p = 0.0143, for correlation between alpha band global coherence(resting state) with precision. Correponding statistics for delta band, rho = 0.0100 and p = 0.8042.

Discussion

Our results indicate distinct changes in global coherence and metastability patterns across the

age continuum. In this section, we relate our findings to existing literature and discuss their possible implications for the understanding of the process of healthy and pathological aging by tracking large scale brain dynamics and frequency specific alterations.

Consistent with extant literature, we find a significant age-related decline in peak alpha frequency. The decrease in peak frequency of alpha band has been reported to be a biomarker of normal and pathological aging process, especially for dementia, mild cognitive impairment, and Alzheimer's disease (Scally et al., 2018; Dickinson et al., 2018; Osipova et al., 2005; Jeong, 2004). Patients with Alzheimer's disease show a significant decrease in peak alpha frequency (PAF) compared to age-matched control group (Osipova et al., 2005; Jeong, 2004). Parkinson's patients with dementia have a lower PAF compared to age-matched controls (Soikkeli et al., 1991). Earlier studies suggest that PAF can be considered to be a robust biomarker of pathology and we observe very similar results in healthy aging. Neurodegenerative pathologies like AD and Parkinson's share many similarities with healthy aging, due to which many have speculated whether neurodegeneration is an accelerated aging process (Ciryam et al., 2016).

Beta oscillations are present in primary motor cortex at rest and get suppressed during movement (Pfurtscheller and Lopes de Silva, 1999). Beta oscillations in motor cortex are thought to be an index of motor inhibition and volitional movement (Heinrichs-Graham and Wilson, 2016). Research also suggests that an increase in intra-cortical GABAergic inhibition gives rise to an increase in resting state beta activity (Hall et al., 2011; Muthukumaraswamy et al., 2013). From this perspective, an increase in beta oscillations in the older population compared to the younger population can be reflective of increased motor inhibition (Heinrichs-Graham et al., 2018). Increase in the band-limited beta power in older population compared to younger population has been reported both in the context of resting state and sensory-motor task (Rossiter et al., 2014; Heinrichs-Graham and Wilson, 2016). We also observed the increase of beta band power with aging (Fig 1. B). Further, it has been reported that resting state band limited activity in slow frequency oscillations, i.e. delta and theta band is typically higher in younger population compared to older population (Volf and Gluhih, 2011). However, we did not observe this on a global level in the present study.

COMMUNICATION THROUGH COHERENCE

Communication through coherence(CTC) hypothesis operationally defines neuronal

17

communication as generation of coherent activity across neuronal assemblies. This view holds that interareal coherence presents windows of excitability where communication channels between brain regions are maximally utilized (Fries, 2005). Resting state brain activity is said to reflect the brain's tendency to engage and disengage these channels of communication spontaneously (Deco et. al, 2011).

From a dynamical perspective, spontaneous brain activity must exhibit metastable dynamics, whereby the global brain dynamic stays clear of the two extremes of constant synchronization and desynchronization and instead, periodically shuttles back and forth between coherent and incoherent regimes. More formally, global coherence indexes the average phase and amplitude correlation across sensors whereas metastability measures the variability in phase relationships of sensors across time. The complimentary, yet related nature of global coherence and metastability offers unique insights into the mechanistic underpinnings of global brain dynamics. An example of this is a recent computational study by Vasa et al. which describes how local lesioning in nodes with high eigenvector centrality leads to a simultaneous decrease in global synchrony along with an increase in metastability. (Vasa et al., 2015). For a review of the complementary nature of global coherence and metastability, see (Deco et al. 2017, Hellyer et al. 2015, Vasa et al. 2015). It is evident how spontaneous metastable brain dynamics would contribute to cognitive flexibility. Since healthy aging exhibits complex changes in cognitive flexibility, we postulated that changes in the brain's resting state metastable dynamics as it ages could be predictive of cognitive flexibility in multitude of task conditions in different representative age groups.

Our earlier work has proposed that a way to implement the CTC hypothesis, that is, optimal exploration of the dynamical repertoire inherent in the brain structural connectivity, is by maximisation of metastability (Deco et. al., 2016). Here, we refer to metastability as a measure of the variability of the states of phase configurations with time. Furthermore, in our previous work we have related CTC with metastability, demonstrating how this idea could be seamlessly explored using fMRI and MEG dynamics combined with whole brain computational models to generate successful predictions. One interesting prediction in this direction is that to maintain spontaneous activity with aging in the face of structural decline, the brain must utilize CTC channels to maximize metastability. This metastability decreases with introduction of external stimulation and task conditions. The flexible selection of different CTC-mediated routes under different task-based conditions requires resting activity to have access to many possible CTC-

18

mediated routes, that is, exhibit a broad exploration of the underlying dynamical repertoire (Deco et. al., 2016). In this key scenario, a ‘gentle’ change triggered by external stimuli or a task can easily bias communication to different CTC-mediated routes. In terms of dynamical systems, this scenario implies that the CTC hypothesis would require the resting brain to exhibit maximal metastability, refining and providing evidence in favour of the synergetic hypothesis of Haken (Corning 1995) (later further explored by Tognoli and Kelso(Tognoli et. al., 2014)).

Interestingly, in our work, the alpha band (8-12 Hz) demonstrates the highest global coherence in any given age group, but whereas alpha metastability increases with age, alpha global coherence reduces with age. Taken together, this would strongly suggest the presence of a primary generator of alpha activity that aids in the maintenance of a brain-wide correlated and synchronized network. The thalamocortical circuitry has long been regarded as the primary generator of activity that falls in the alpha band (Pfurtscheller and Lopes de Silva, 1999). Interestingly, a somewhat different trend is seen in the delta and theta band, where we notice an age-related increase in global coherence and metastability. We also notice inflection points in the life span profiles of global coherence around the age of 20-30 and 70-80 in both the slower and faster bands.

We observe an age-related increase in global metastability across all frequency bands under study here. Moreover, our results reveal a differential profile of relative metastability in the slower and faster frequencies as a consequence of aging. We want to discuss these results in the light of two opposing theories of healthy aging. The method of neuro-compensation argues that age-related changes in brain dynamics suggest a compensatory mechanism by which function gets restored in response to structural decline (Naik et al. 2017). In this regard, it is interesting to note that Alzheimer’s disease and Traumatic brain injuries are associated with a reduction in global metastability (Córdova-Palomera et al., 2017; Hellyer et al., 2015). Since metastability is a direct measure of the functional capacity of the brain and has been shown to confer cognitive flexibility in task-switching, information-processing and logical memory (Hellyer et al. 2015), this would argue in favour of a compensatory explanation of the global increase in metastability with aging. However, the neural noise hypothesis of aging would suggest a different interpretation. This theory argues that age-related cognitive decline is best explained as a consequence of an increase in the noisy baseline activity of the brain (Voytek et al., 2015;

Dave et al., 2018). According to this framework, global phase inconsistencies would arise as a result of an age-related increase in neural noise. Within this framework, changes in global metastability and coherence reflect an epiphenomenon that occurs due to an increase in neural noise. Future efforts should focus on resolving this debate. One possible direction would be to study brain signals through measures of signal complexity using source reconstructed EEG/MEG, to elucidate the role of specific brain regions in bringing about metastable patterns of activity. More direct estimates of metastable state switching from electrophysiological data could be employed to disentangle the effects of noise. Recent papers have proposed ways to directly estimate metastable switching between synchrony states. For example, Vidaurre et. al. (Vidaurre et.al. 2016) propose a Hidden Markov Model based method to decompose electrophysiological time series into recurrent, quasi-stationary phase-locked regimes. This involves fitting source reconstructed time series with multivariate autoregressive models and modelling state switches through a hidden markov approach. Another promising avenue would be to invoke whole brain computational models which incorporate neural plasticity mechanisms that operate at time scales that are relevant to aging (Abeysuriya et al., 2018).

RELATIONSHIP TO COGNITION

Both global coherence and metastability results suggest the emergence of a temporal dichotomy between slower and faster frequencies with age. The average coherence in the lower frequencies increases whereas it decreases for the faster frequencies with age. Similarly, faster time scales are associated with higher metastability as compared to slower time scales in the younger population whereas the reverse is true for the older population. We interpret this observation of a split in slow and fast time scales by making two observations. Firstly, while the process of ageing is marked by a decline in various cognitive faculties, some higher level cognitive faculties remain preserved, or even improve with ageing. For example, while fluid intelligence (the ability to find solutions to novel problems, not requiring prior knowledge) is found to be higher in younger adults, there is evidence to suggest that crystallized intelligence (ability to use prior knowledge for problem solving) increases with age. Similarly, there is evidence indicating an improvement in discourse skills with ageing; older adults form better structured narratives than younger adults. Other linguistic abilities like vocabulary, grammatical judgement and repetition ability are found to remain stable with age. Secondly, years of research in cognitive neuroscience has established a mapping between various cognitive processes and specific oscillatory frequency bands. For example, while memory processes are

associated with theta rhythms, attentional processes are most related to alpha rhythms. Our findings raise the possibility that the differential changes in band specific global coherence and metastability may be indicating a compensatory functional reorganization of the brain, wherein cognitive functions mediated by slower frequencies are preserved through an increase in the underlying coherence and relative metastability.

Future effort should aim to explicitly link behavioural scores with indices of band specific global coherence and metastability to address this question.

THEORIES OF AGEING

Various theories have been expounded to explain cognitive functions with age. Theories such as HAROLD (Hemispheric asymmetry reduction in older adults), PASA (posterior to anterior shift with age) and CRUNCH (Compensation related utilization of neural circuit hypothesis) characterize ageing on the basis of topographical changes in activation patterns during task conditions. On the other hand theories like DECHA (default to executive coupling hypothesis with age) look at age associated changes as arising from impaired connectivity between specific functional modules in the brain(Naik et al. 2017). The latter approach emphasises the network dimension, whereas, the former approach confines itself to tracking changes in gross patterns of activation contingent upon tasks. However, the latter approach suffers from various methodological hurdles such as extensive processing to extract meaningful resting state networks and the concomitant individual variability. Here we sought to take a middle path by focusing on easy to extract metrics such as coherence and metastability that are also appropriate surrogates for underlying functional couplings. Additionally, these metrics have the added advantage of providing frequency specific information unlike BOLD signals that are temporally restricted. Future effort will look to validate these metrics against direct estimates for metastable state switching.

METHODOLOGICAL LIMITATIONS

21

We would also like to draw attention to some limitations of the current study. Since the current analysis is restricted to the sensor level, our results are so far only indicative of activity at the neural level. Source reconstruction may provide a direct estimate of global coherence at the level of neural assemblies and help in elucidating its relationship with sensor level global coherence. Caution is also required in interpreting the results due to the modest effect sizes involved. Similarly, caution is warranted in interpreting global coherence and metastability measures. Due to the way it is constructed, global coherence may give misleading information under some circumstances. For example, it is possible to obtain spuriously high values of global coherence even when the underlying signals are independent when most of the power is concentrated in a few sensors. In this study, the almost evenly distributed scalp topographies(Fig.3) would preclude that possibility. Similarly, there could exist pathological phase relationships that could be missed due to the way we estimate metastability. For example, if a metastable state corresponds to a anti-phasic relationship between all oscillators, the resulting standard deviation of the order parameter would be close to zero. Therefore, such metastable dynamics would not be picked up by this approach. Since the CTC hypothesis assumes phase locked regimes to be the substrate of neural communication, using the standard deviation of kurmaoto order parameter as a proxy for metastability would serve our purpose. Future work is underway to address some of these issues.

Here it is essential to point out that the results are pointing towards the existence of a temporal dichotomy between slow and fast time scales in both global coherence and metastability but the exact extents of the beta band are different for the two cases. While global coherence utilizes 16-25 Hz as beta, the dichotomous effect in metastability is seen in 24-28 Hz and 30-32 Hz range and is noticed as statistically significant only between the extreme groups(delta, theta versus beta 4, beta 5). This slight difference could be due to differences in the signal processing steps leading up to the calculation of global coherence and metastability-while global coherence relies on fourier transforms to extract cross spectrum, metastability analysis requires explicit band pass filtering in bands of interest prior to hilbert transform based phase extraction. We would like to point out that we have devised our own definition for beta band for convenient phase estimation; the beta bands considered here are different from other classifications such as Rangaswamy et.al.(Rangaswamy et. al., 2002) which uses similar terminology as us(beta 1,2,3).

In summary, we propose the validity of studying ageing under the CTC framework as it provides a link between cognition and oscillations, both of which undergo significant alterations with age. Viewed within this framework, our observation of an increase in metastability with age would suggest a homeostatic re-adjustment of the CTC mediated communication channels to compensate for the cognitively deleterious effects of structural decline with age. Further work to link coherence and metastability with direct measures of cognition would help in elucidating the relationship of coherent communication and behaviour and how they evolve with age.

Conclusions

In summary, our analysis reveals the spatiotemporal relationship of resting state spectral signals with healthy aging. In addition, we also demonstrate the age-related changes in global patterns of activity measured through global coherence and metastability. We discuss the subtle relationship between healthy aging and age-related neuropathologies. Future effort should address the issue of whether the multi-factorial space consisting of spectral powers, peak alpha frequency, global coherence, and metastability can improve the accuracies of classifiers that aim to segregate healthy aging from neurodegenerative disorders. Analysis of the spectrotemporal changes associated with aging also holds the promise of furthering our understanding of age-related neuro-compensatory mechanisms and resolving long-standing debates on the nature of brain aging.

Disclosure Statement

The authors declare no conflicts of interest.

Acknowledgements

This study was supported by NBRC Core funds, Ramalingaswami Fellowships (Department of Biotechnology, Government of India) to DR (BT/RLF/Re-entry/07/2014) and AB (BT/RLF/Re-entry/31/2011) and Innovative Young Biotechnologist Award (IYBA) to AB (BT/07/IYBA/2013). AB also acknowledges the support of Centre of Excellence in Epilepsy and MEG. DR was also supported by SR/CSRI/21/2016 extramural grant from the Department of Science and

Technology (DST) Ministry of Science and Technology, Government of India. Data collection and sharing for this project was provided by the Cambridge Centre for Ageing and Neuroscience (CamCAN). CamCAN funding was provided by the UK Biotechnology and Biological Sciences Research Council (grant number BB/H008217/1), together with support from the UK Medical Research Council and University of Cambridge, UK. In accordance with the data usage agreement for CAMCAN dataset, the article has been submitted as open-access.

References

Abeysuriya, R. G., Hadida, J., Sotiropoulos, S. N., Jbabdi, S., Becker, R., Hunt, B. A., ... & Woolrich, M. W. (2018). A biophysical model of dynamic balancing of excitation and inhibition in fast oscillatory large-scale networks. *PLoS computational biology*, *14*(2), e1006007.

Benjamini, Y., Hochberg, Y. (1995). Controlling the false discovery rate: A practical and powerful approach to multiple testing. J. R. Stat. Soc. Series B Stat. Methodol. 57, 289-300.

Bishop, N. A., Lu, T., & Yankner, B. A. (2010). Neural mechanisms of ageing and cognitive decline. *Nature*, *464*(7288), 529.

Bokil, H., Andrews, P., Kulkarni, J. E., Mehta, S., & Mitra, P. P. (2010). Chronux: a platform for analyzing neural signals. *Journal of neuroscience methods*, *192*(1), 146-151.

Bressler, S. L., & Kelso, J. S. (2001). Cortical coordination dynamics and cognition. Trends in cognitive sciences, *5*(1), 26-36.

Buzsaki, G.(2011) Rhythms of the brain. Oxford University Press

Cimenser,A.,Purdon,P.L.,Pierce,E.T.,Walsh,J.L.,Salazar-Gomez,A.F.,

Dave, S., Brothers, T. A., & Swaab, T. Y. (2018). 1/f neural noise and electrophysiological indices of contextual prediction in aging. *Brain research*, *1691*, 34-43.

Clark, C. R., Veltmeyer, M. D., Hamilton, R. J., Simms, E., Paul, R., Hermens, D., & Gordon, E. (2004). Spontaneous alpha peak frequency predicts working memory performance across the

age span. International Journal of Psychophysiology, *53*(1), 1-9.

Córdova-Palomera, A., Kaufmann, T., Persson, K., Alnæs, D., Doan, N. T., Moberget, T., & Engedal, K. (2017). Disrupted global metastability and static and dynamic brain connectivity across individuals in the Alzheimer's disease continuum. Scientific reports, *7*, 40268.

Corning, P. A. (1995). Synergy and self-organization in the evolution of complex systems. *Systems Research*, *12*(2), 89-121.

Davis, S. W., Dennis, N. A., Daselaar, S. M., Fleck, M. S., Cabeza, R. (2008). Que PASA? The posterior-anterior shift in aging. Cereb. Cortex. 18, 1201–1209.

Davis, S. W., Dennis, N. A., Buchler, N. G., White, L. E., Madden, D. J., & Cabeza, R. (2009). Assessing the effects of age on long white matter tracts using diffusion tensor tractography. *Neuroimage*, *46*(2), 530-541.

Deco, G., Jirsa, V.K., McIntosh, A.R. (2011). Emerging concepts for the dynamical organization of resting-state activity in the brain. Nat. Rev. Neurosci. 12, 43-56.

Deco, G., & Kringelbach, M. L. (2016). Metastability and coherence: extending the communication through coherence hypothesis using a whole-brain computational perspective. *Trends in neurosciences*, *39*(3), 125-135.

Deco, G., Cabral, J., Woolrich, M. W., Stevner, A. B., Van Hartevelt, T. J., & Kringelbach, M. L. (2017). Single or multiple frequency generators in on-going brain activity: A mechanistic whole-brain model of empirical MEG data. *Neuroimage*, *152*, 538-550.

Dickinson, A., DiStefano, C., Senturk, D., & Jeste, S. S. (2018). Peak alpha frequency is a neural marker of cognitive function across the autism spectrum. *European Journal of Neuroscience*, *47*(6), 643-651.

Duffy, F.H., Albert, M.S., McAnulty, G., Garvey, AJ. (1984). Age-related differences in brain electrical activity of healthy subjects. Ann. Neurol. 16, 430-438.

Foster, J. J., Sutterer, D. W., Serences, J. T., Vogel, E. K., & Awh, E. (2015). The topography of alpha-band activity tracks the content of spatial working memory. *Journal of neurophysiology*, *115*(1), 168-177.

Fotenos, A.F., Snyder, A.Z., Girton, L.E., Morris, J.C., Buckner, R.L. (2005). Normative estimates of cross-sectional and longitudinal brain volume decline in aging and AD. Neurology. 64, 1032-1039.

Fries, P. (2005). A mechanism for cognitive dynamics: neuronal communication through neuronal coherence. Trends Cogn. Sci. 9, 474-480.

Hall, S.D., Stanford, I.M., Yamawaki, N., McAllister, C.J., Rönnqvist, K.C., Woodhall, G.L., Furlong, P.L. (2011). The role of GABAergic modulation in motor function related neuronal network activity.

Hanslmayr, S., Aslan, A., Staudigl, T., Klimesch, W., Herrmann, C.S., Bäuml, K.H. (2007). Prestimulus oscillations predict visual perception performance between and within subjects. Neuroimage. 37, 1465-1473.

Harrell,P.G., et. al.(2011).Tracking brain states under general anesthesia by Using global coherence analysis. Proc.Natl.Acad.Sci.U.S.A. 108,8832–8837.
doi:10.1073/pnas

Heinrichs-Graham, E., McDermott, T. J., Mills, M. S., Wiesman, A. I., Wang, Y. P., Stephen, J. M., ... & Wilson, T. W. (2018). The lifespan trajectory of neural oscillatory activity in the motor system. Developmental cognitive neuroscience, *30*, 159-168.

Hellyer, P. J., Scott, G., Shanahan, M., Sharp, D. J., & Leech, R. (2015). Cognitive flexibility through metastable neural dynamics is disrupted by damage to the structural connectome. *Journal of Neuroscience*, *35*(24), 9050-9063.

Ishii, R., Canuet, L., Aoki, Y., Hata, M., Iwase, M., Ikeda, S., ... & Ikeda, M. (2017). Healthy and Pathological Brain Aging: From the Perspective of Oscillations, Functional Connectivity, and Signal Complexity. *Neuropsychobiology*, *75*(4), 151-161.

JF Hipp, DJ Hawellek, M Corbetta, M Siegel, AK Engel (2012) Large-scale cortical correlation structure of spontaneous oscillatory activity. Nature Neuroscience volume 15, pages 884–890.

Jeong, J. (2004). EEG dynamics in patients with Alzheimer's disease. Clin. Neurophysiol. 115, 1490-1505.

Kempermann, G., Kuhn, H.G., Gage, F.H. (1997). More hippocampal neurons in adult mice living in an enriched environment. Nature. 386, 493-505.

Koenig, T., Prichep, L., Lehmann, D., Sosa, P.V., Braeker, E., Kleinlogel, H., Isenhart, R., John, E.R. (2002). Millisecond by millisecond, year by year: normative EEG microstates and developmental stages. Neuroimage. 16, 41-48.

Kringelbach, M. L., McIntosh, A. R., Ritter, P., Jirsa, V. K., & Deco, G. (2015). The rediscovery of slowness: exploring the timing of cognition. *Trends in cognitive sciences*, *19*(10), 616-628.

Kumar, G. V., Halder, T., Jaiswal, A. K., Mukherjee, A., Roy, D. and Banerjee, A. (2016). Large scale functional brain networks underlying temporal integration of audio–visual speech perception: An EEG study, Front. Psychol. 7, 1558. DOI:10.3389/fpsyg.2016.01558.

Loerch, P. M., Lu, T., Dakin, K. A., Vann, J. M., Isaacs, A., Geula, C., ... & Prolla, T. A. (2008). Evolution of the aging brain transcriptome and synaptic regulation. *PloS one*, *3*(10), e3329.

Maurits, N.M., Scheeringa, R., van der Hoeven, J.H., de Jong, R. (2006). EEG coherence obtained from an auditory oddball task increases with age. J. Clin. Neurophysiol. 23, 395-403.

Muthukumaraswamy, S.D., Myers, J.F., Wilson, S.J., Nutt, D.J., Lingford-Hughes, A., Singh, K.D., Hamandi, K. (2013). The effects of elevated endogenous GABA levels on movement-related network oscillations. Neuroimage. 66, 36-41.

Naik, S., Banerjee, A., Bapi, R.S., Deco, G., Roy, D. (2017). Metastability in Senescence. Trends Cogn. Sci. 21, 509-527.

Osipova, D., Ahveninen, J., Jensen, O., Ylikoski, A., Pekkonen, E. (2005). Altered generation of

spontaneous oscillations in Alzheimer's disease. Neuroimage. 27, 835-841.

Oostenveld, R., Fries, P., Maris, E., & Schoffelen, J. M. (2011). FieldTrip: open source software for advanced analysis of MEG, EEG, and invasive electrophysiological data. *Computational intelligence and neuroscience*, *2011*, 1.

Pesaran, B., Vinck, M., Einevoll, G. T., Sirota, A., Fries, P., Siegel, M., Truccolo, W., Schroeder, C. E.,Srinivasan, R. (2018) Investigating Large-Scale Brain Dynamics Using Field Potential Recordings: Analysis and Interpretation. *Nature Neuroscience*. **21**, 903–919.

Pfefferbaum, A., Sullivan, E. V., Hedehus, M., Lim, K. O., Adalsteinsson, E., & Moseley, M. (2000). Age-related decline in brain white matter anisotropy measured with spatially corrected echo-planar diffusion tensor imaging. *Magnetic Resonance in Medicine: An Official Journal of the International Society for Magnetic Resonance in Medicine*, *44*(2), 259-268.

Pfurtscheller, G., Lopes da Silva, F.H. (1999). Event-related EEG/MEG synchronization and desynchronization: basic principles. Clin. Neurophysiol. 110, 1842-1857.

Purdon, P.L., Pavone, K.J., Akeju, O., Smith, A.C., Sampson, A.L., Lee, J., Zhou, D.W., Solt, K., Brown, E.N. (2015). The Ageing Brain: Age-dependent changes in the electroencephalogram during propofol and sevoflurane general anaesthesia. Br. J. Anaesth. 115, i46-i57.

Rangaswamy, M., Porjesz, B., Chorlian, D. B., Wang, K., Jones, K. A., Bauer, L. O., ... & Begleiter, H. (2002). Beta power in the EEG of alcoholics. *Biological psychiatry*, *52*(8), 831-842.

Raz, N., Lindenberger, U., Rodrigue, K. M., Kennedy, K. M., Head, D., Williamson, A., ... & Acker, J. D. (2005). Regional brain changes in aging healthy adults: general trends, individual differences and modifiers. *Cerebral cortex*, *15*(11), 1676-1689.

Reuter-Lorenz, P.A., Jonides, J., Smith, E.E., Hartley, A., Miller, A., Marshuetz, C., Koeppe, R.A. (2000). Age differences in the frontal lateralization of verbal and spatial working memory revealed by PET. J. Cogn. Neurosci. 12, 174-187.

Rossini, P.M., Del Percio, C., Pasqualetti, P., Cassetta, E., Binetti, G., Dal Forno, G., Ferreri, F.,

Frisoni, G., Chiovenda, P., Miniussi, C., Parisi, L., Tombini, M., Vecchio, F., Babiloni, C. (2003). Conversion from mild cognitive impairment to Alzheimer's disease is predicted by sources and coherence of brain electroencephalography rhythms. Neuroscience. 143, 793-803.

Rossiter, H.E., Davis, E.M., Clark, E.V., Boudrias, M.H., Ward, N.S. (2014). Beta oscillations reflect changes in motor cortex inhibition in healthy ageing. Neuroimage. 91, 360-365.

Samaha, J., & Postle, B. R. (2015). The speed of alpha-band oscillations predicts the temporal resolution of visual perception. Current Biology, *25*(22), 2985-2990.

Samaha, J., Sprague, T. C., & Postle, B. R. (2016). Decoding and reconstructing the focus of spatial attention from the topography of alpha-band oscillations. *Journal of cognitive neuroscience*, *28*(8), 1090-1097.

Scally, B., Burke, M. R., Bunce, D., & Delvenne, J. F. (2018). Resting-state EEG power and connectivity are associated with alpha peak frequency slowing in healthy aging. *Neurobiology of aging*, *71*, 149-155.

Shafto, M.A., Tyler, L.K., Dixon, M., Taylor, J.R., Rowe, J.B., Cusack, R., Calder, A.J., Marslen-Wilson, W.D., Duncan, J., Dalgleish, T., Henson, R.N., Brayne, C., CamCAN, & Matthews, F.E. (2014). The Cambridge Centre for Ageing and Neuroscience (CamCAN) study protocol: a cross-sectional, lifespan, multidisciplinary examination of healthy cognitive ageing. BMC Neurology, 14(204). doi:10.1186/s12883-014-0204-1.

Soikkeli, R., Partanen, J., Soininen, H., Pääkkönen, A., Riekkinen, P.Sr. (1991). Slowing of EEG in Parkinson's disease. Electroencephalogr. Clin. Neurophysiol. 79, 159-165.

Stam, C.J., van der Made, Y., Pijnenburg, Y.A., Scheltens, P. (2003). EEG synchronization in mild cognitive impairment and Alzheimer's disease. Acta. Neurol. Scand. 108, 90-96.

Strunk, J., James, T., Arndt, J., Duarte, A. (2017). Age-related changes in neural oscillations supporting context memory retrieval. Cortex. 91, 40-55.

Taulu, S., Simola, J., Kajola, M. (2005). Applications of the signal space separation method.

IEEE Trans. Signal Process. 53, 3359-3372.

Taylor, J.R., Williams, N., Cusack, R., Auer, T., Shafto, M.A., Dixon, M., Tyler, L.K., Cam-CAN, Henson, R.N. (2017). The Cambridge Centre for Ageing and Neuroscience (Cam-CAN) data repository: Structural and functional MRI, MEG, and cognitive data from a cross-sectional adult lifespan sample. NeuroImage. 144, 262-269.

Toepper, M. (2017). Dissociating normal aging from Alzheimer's disease: A view from cognitive neuroscience. *Journal of Alzheimer's Disease*, *57*(2), 331-352.

Tognoli, E., & Kelso, J. S. (2014). The metastable brain. *Neuron*, *81*(1), 35-48.

Uhlhaas, P.J., Singer, W. (2006). Neural Synchrony in Brain Disorders: Relevance for Cognitive Dysfunctions and Pathophysiology. Neuron. 52, 155-168.

Vidaurre, D., Quinn, A. J., Baker, A. P., Dupret, D., Tejero-Cantero, A., & Woolrich, M. W. (2016). Spectrally resolved fast transient brain states in electrophysiological data. *Neuroimage*, *126*, 81-95.

Volf, N.V., Gluhih, A.A. (2011). Background cerebral electrical activity in healthy mental aging. Hum. Physiol. 37, 51-60

Voytek, B., Kramer, M. A., Case, J., Lepage, K. Q., Tempesta, Z. R., Knight, R. T., & Gazzaley, A. (2015). Age-related changes in 1/f neural electrophysiological noise. *Journal of Neuroscience*, *35*(38), 13257-13265.

Zhang, W., & Luck, S. J. (2008). Discrete fixed-resolution representations in visual working memory. *Nature*, *453*(7192), 233.

Table and Figure Legends

Table1. Sample size and gender in each representative age group

Figure 1. Relation between global spectral activity and age. A. Plots of mean power spectral density for 4 non-overlapping age groups i.e. 18-35, 36-50, 51-65 and 66-88. Shaded region denotes standard error of mean. **B.** Boxplot of distribution of band limited power in the beta band (16-25 Hz). Blue line indicates the median of each distribution. Notch denotes 95%

30

confidence interval of the median. **C.** Variation of alpha activity with aging. Center frequency in the alpha band for each age bin has been plotted as solid circles and solid black line is the linear fit of these points(labels indicate effect sizes,significance and correlation function) **D.** Sensor topography of correlation between peak alpha frequency and age. Colorbar represents Spearman's rank correlation value.

Figure 2. Differential changes in global coherence with aging. **A.** Plots of mean global coherency for the four age groups. Shaded region denotes s.e.m. **B.** Differential variation of global coherency for slow (1-5 Hz) and fast oscillations (10-20 Hz). **C.** Variation of global coherence with aging. Solid circle denote the average global coherence value for a) Delta oscillations (1-3 Hz) b) Theta oscillations (3-7 Hz) c) Alpha oscillations (8-12 Hz) d) Beta oscillations (16-25 Hz) in each age bin of 5 years. Errorbar denotes s.e.m

Figure 3. Segregation of sensor level topographies with aging. **A.** Sensor topographies of alpha power at center frequency and average beta power for the two extreme age groups. **B.** Clusters of sensors with significant differences in power between the oldest and youngest age group for alpha band (8-12 Hz) and beta band (16-25 Hz). White dots represent sensors with a negative difference and black dots represent sensors with a positive difference. **C.** Boxplot for the distribution of angles between the sensor topographies of center alpha power and average beta power for the four age groups. Blue line denotes the median of the distribution and the notch indicates 95% confidence interval of the median.

Figure 4:Metastability across age groups. A. Metastability of four age groups. **B.** Metastability of the four age groups in the delta, theta and alpha bands. Stars between bars indicate statistical significance. **C.** Metastability across age groups divided into age bands of 5 years. **D.** Differential profiles of metastability in young vs old cohort. Statistical significance (indicated by stars) between slow frequencies (delta and theta) and fast frequencies- beta 4(24-28 Hz) and beta 5(28-32Hz) for single two-sample KS test.

Figure 5: Region-wise increase and decrease in global metastability. A. Shows the results for the region-wise metastability analysis. Colors indicate the direction of the age-related trend as measured by the spearman rank correlation coefficients. 14 sensors were chosen at random from each of the 5 anatomical areas- frontal, centro-parietal, occipital, left and right temporal. **B.** Vector View magnetometer layout.

Figure 6: Correlation of VSTM precision with global coherence. A. Scatterplot of precision with age. **B.** Scatterplot of global coherence in alpha band with precision in VSTM task.

Figure 1.

A. Global Spectrum of different age groups

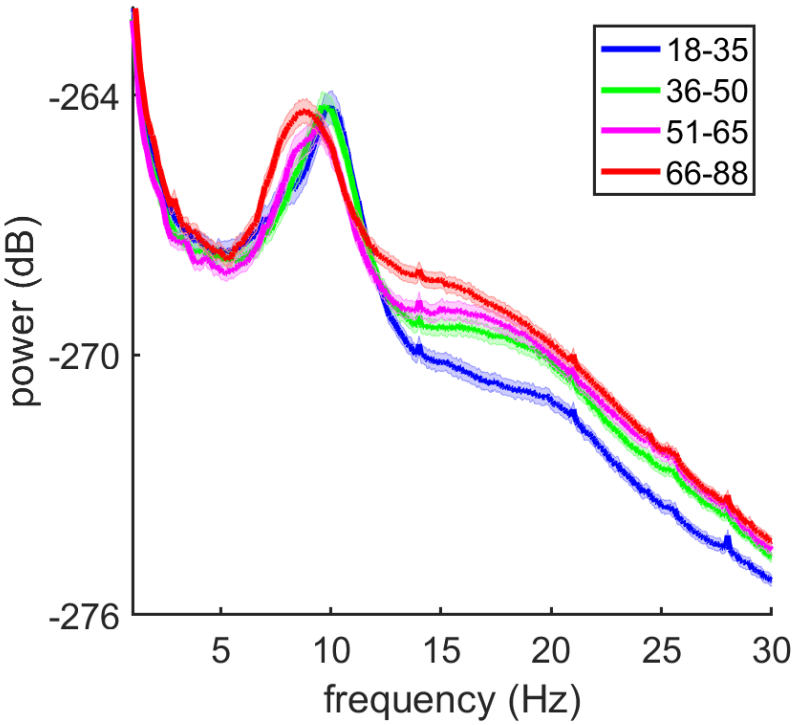

B. Variation in Beta power with age

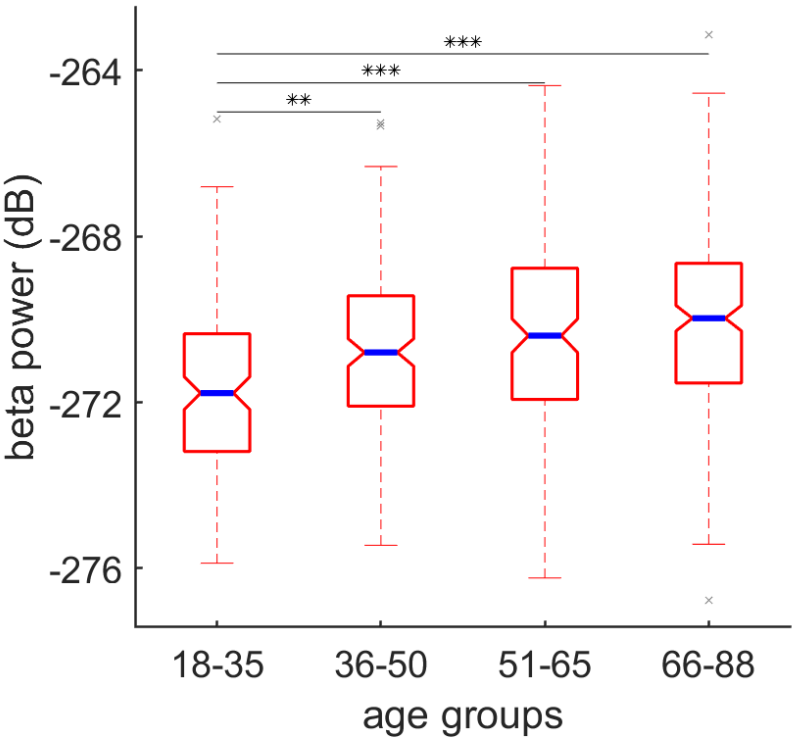

C. Alpha power with age

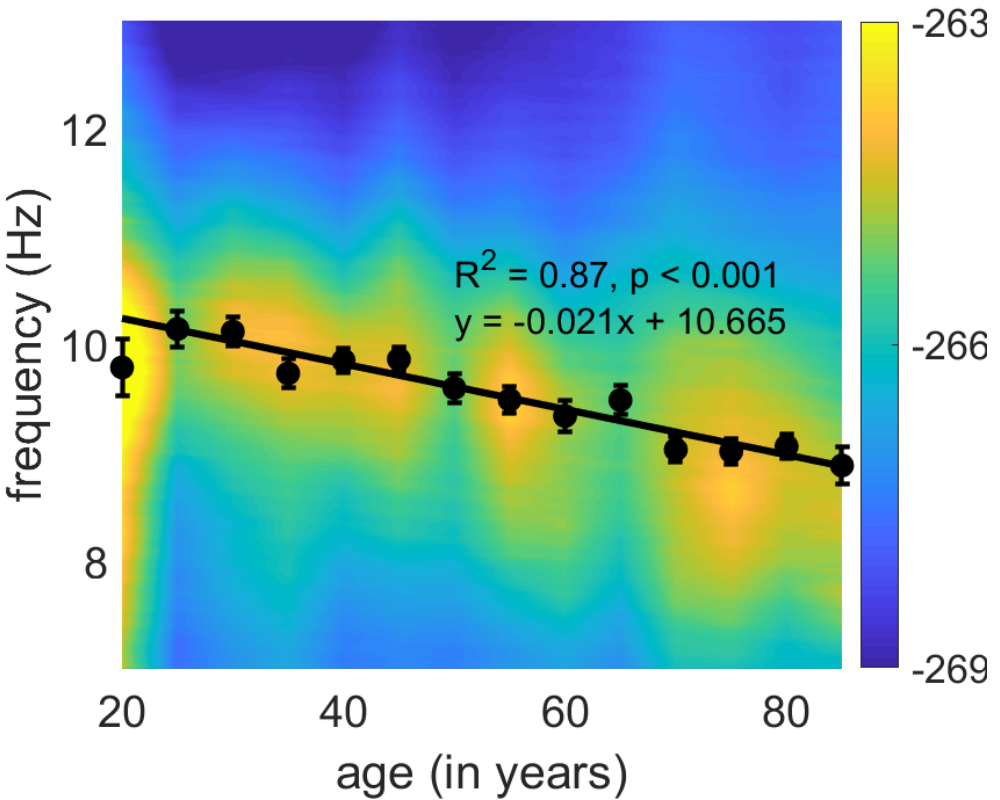

D. Sensor-wise correlation of PAF with age

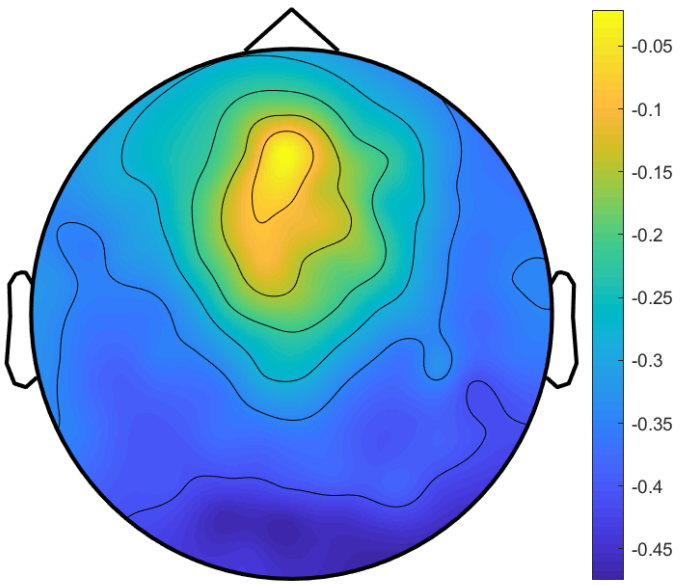

Figure 2.

A. Global Coherence of Different Age Groups

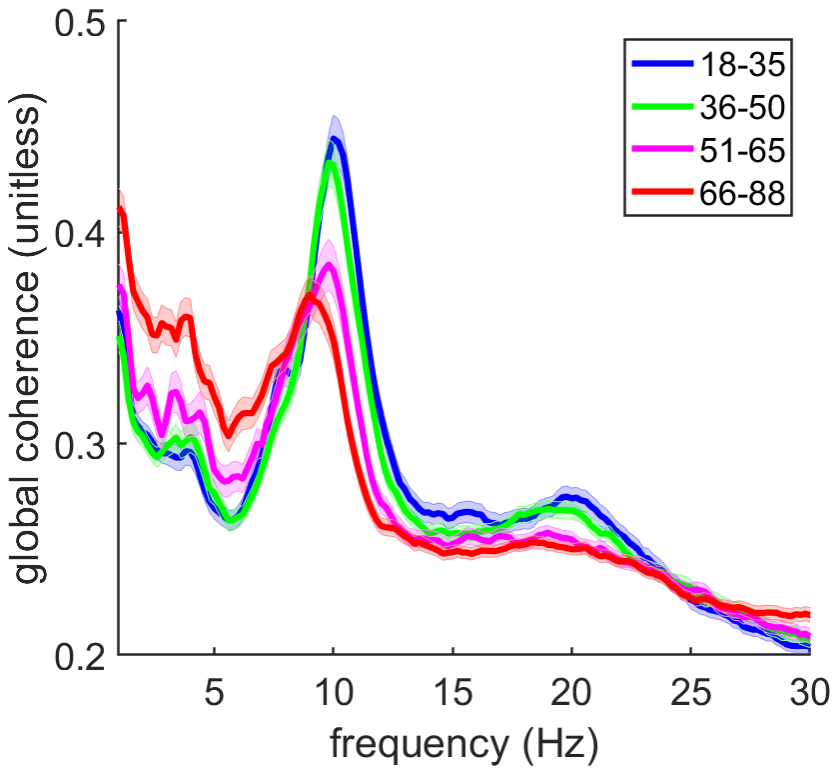

B. Global Coherence of Oscillations at slow and fast time scales.

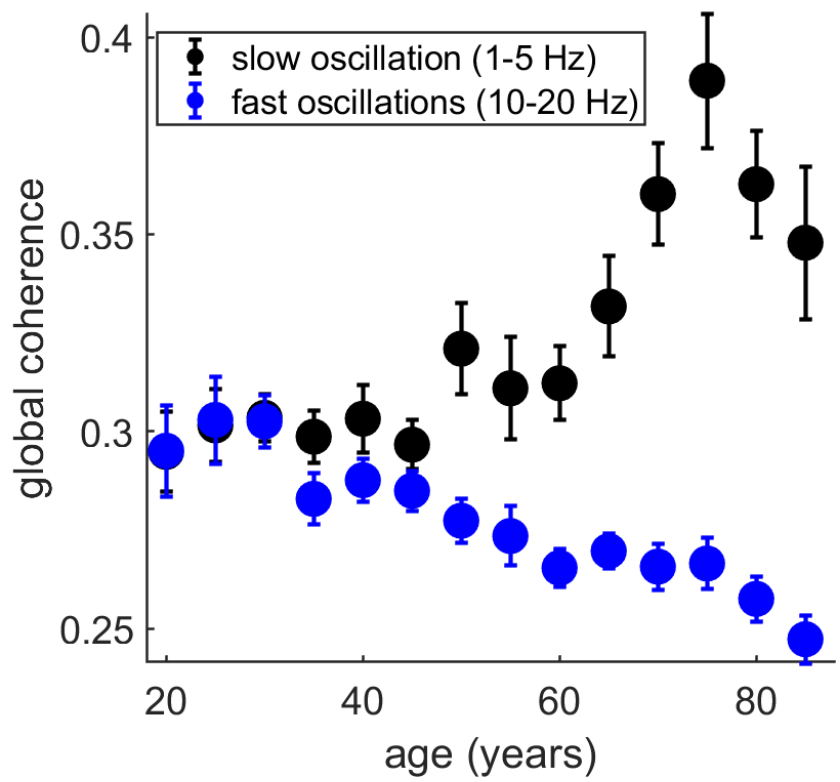

C. Global Coherence in different frequency bands

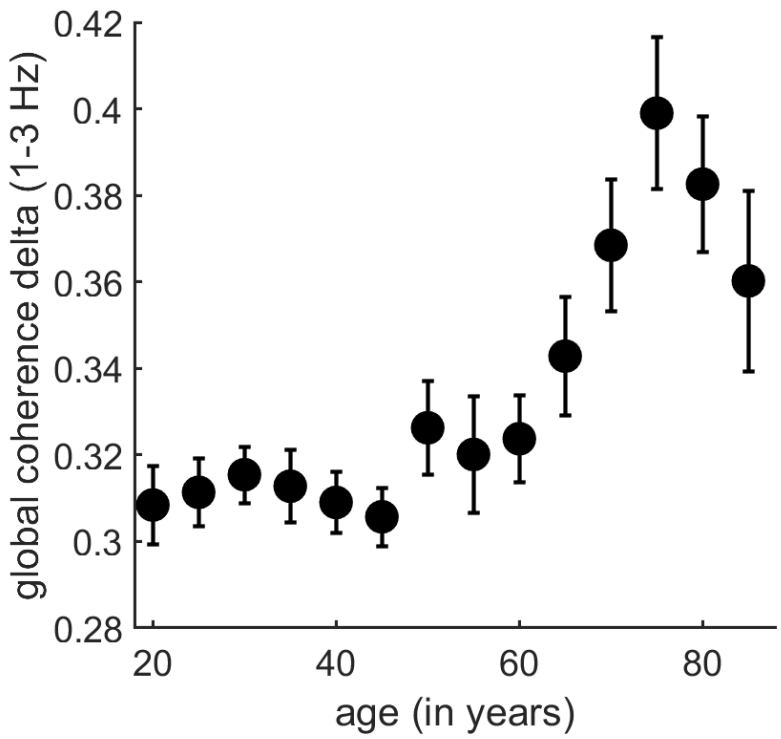

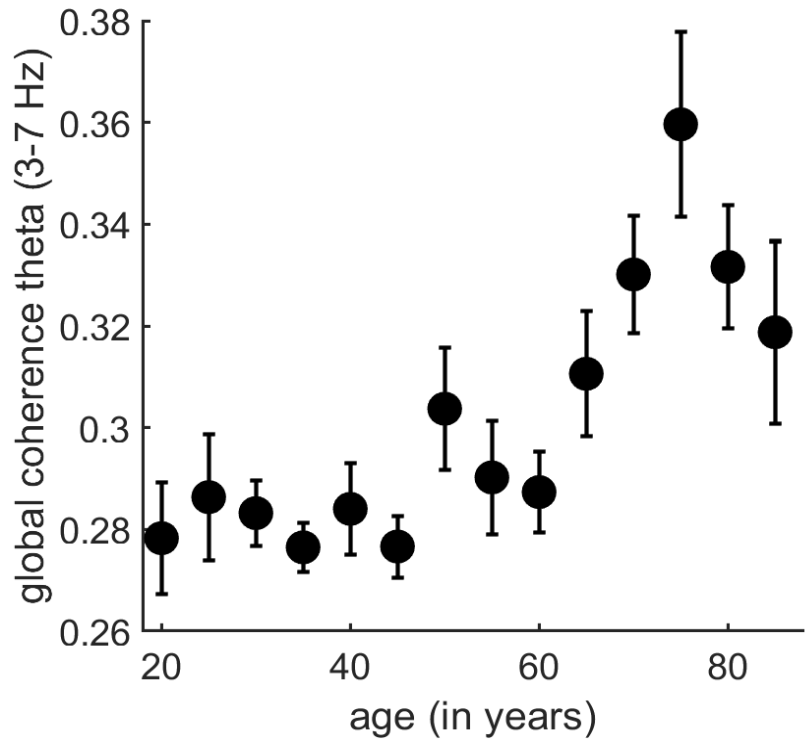

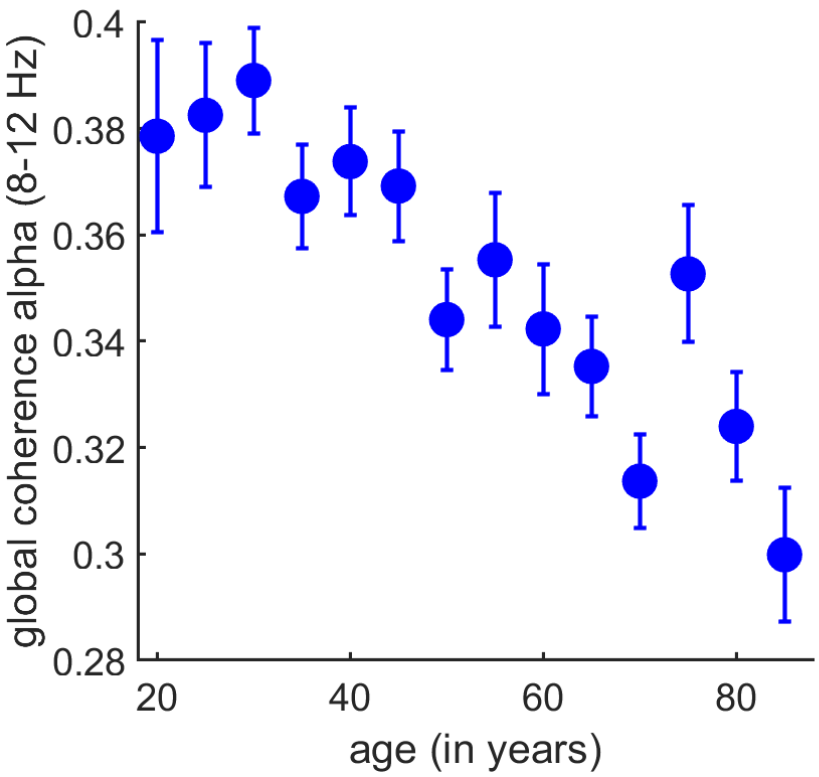

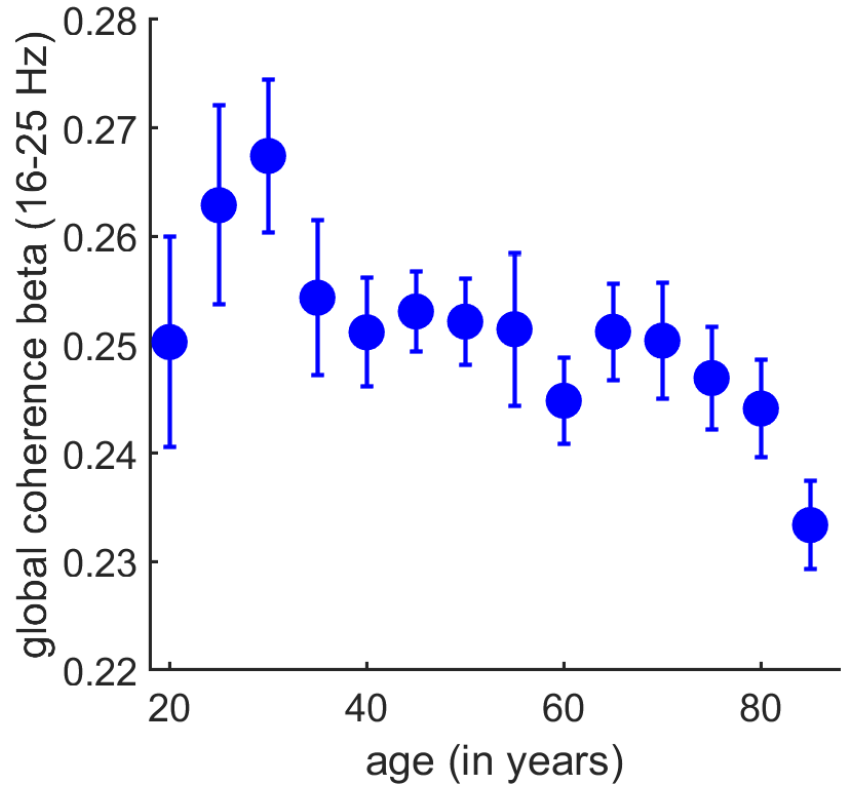

Figure 3.

A. Topographical representation for YA and OA

B. Cluster of sensors showing differences between YA and OA

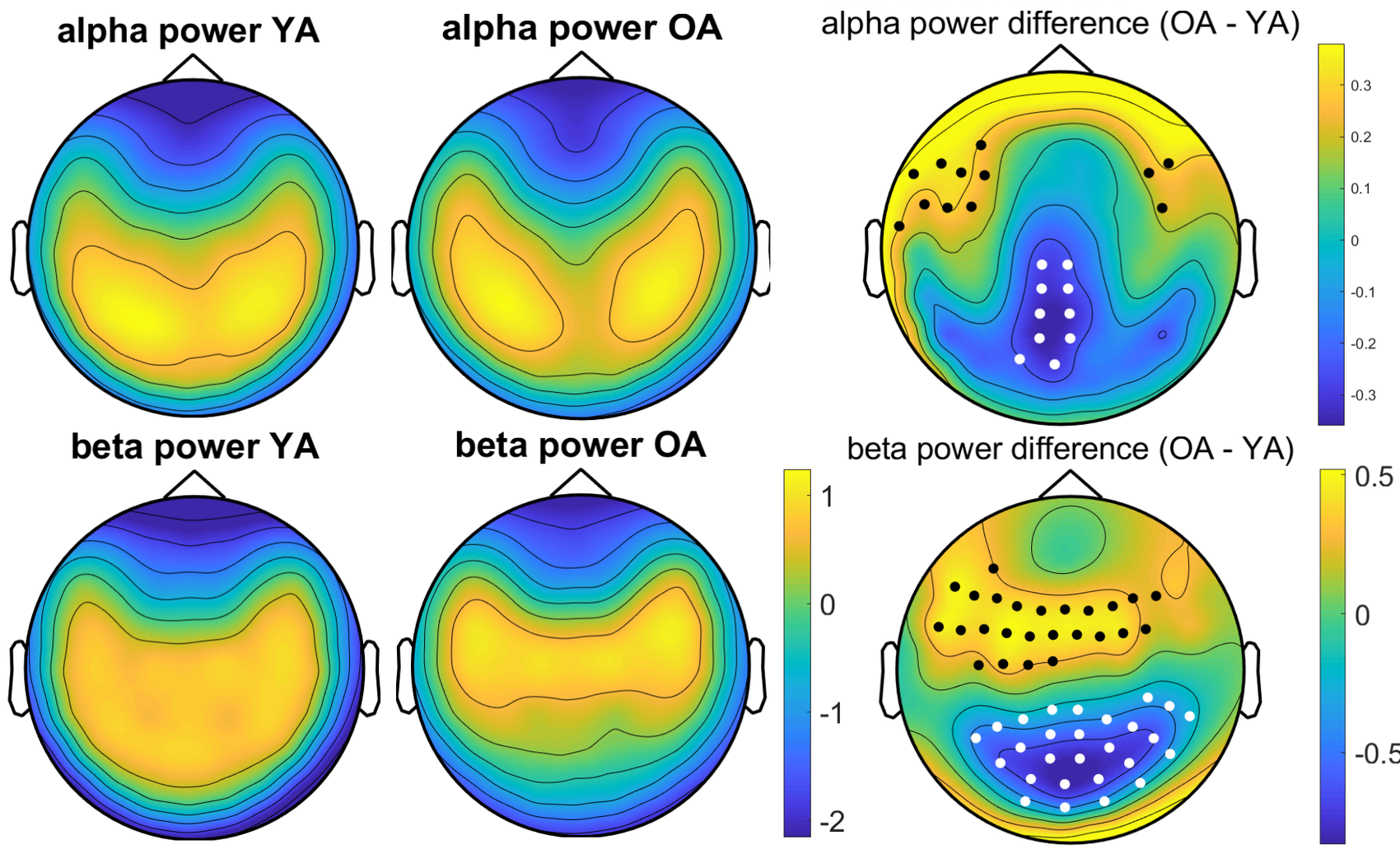

C. Variation in alpha and beta sensor map with ageing

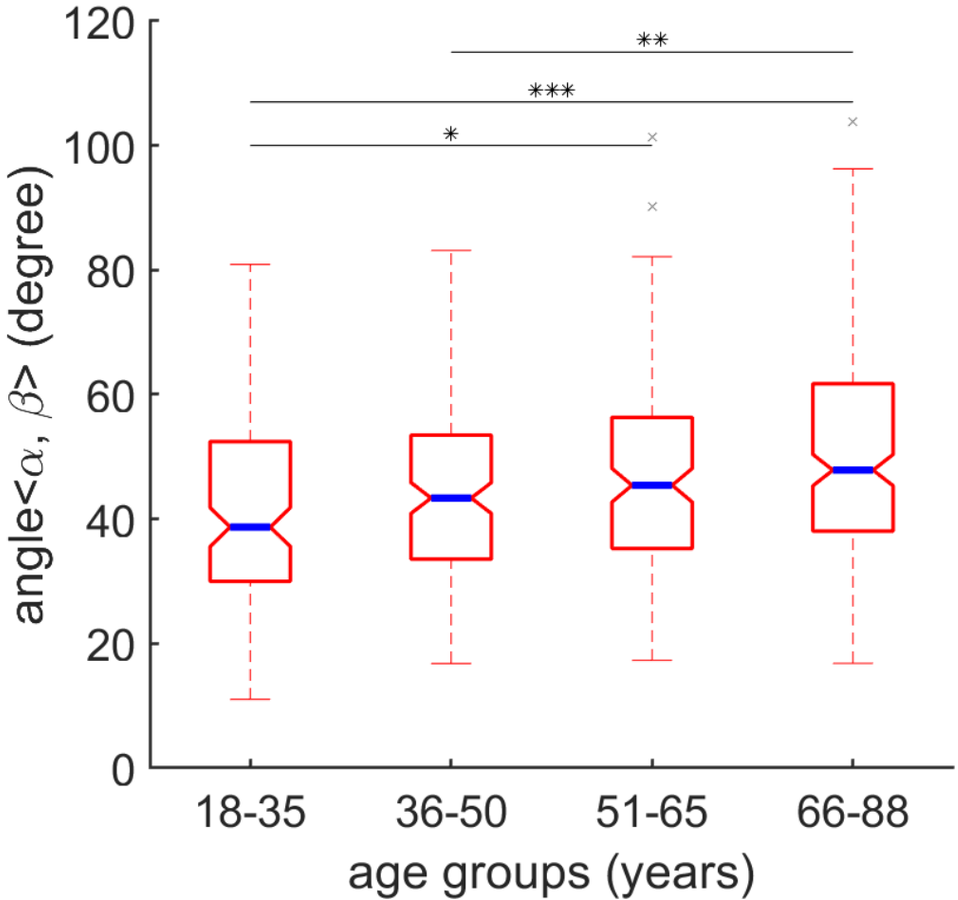

Figure 4.

A.Metastability with ageing

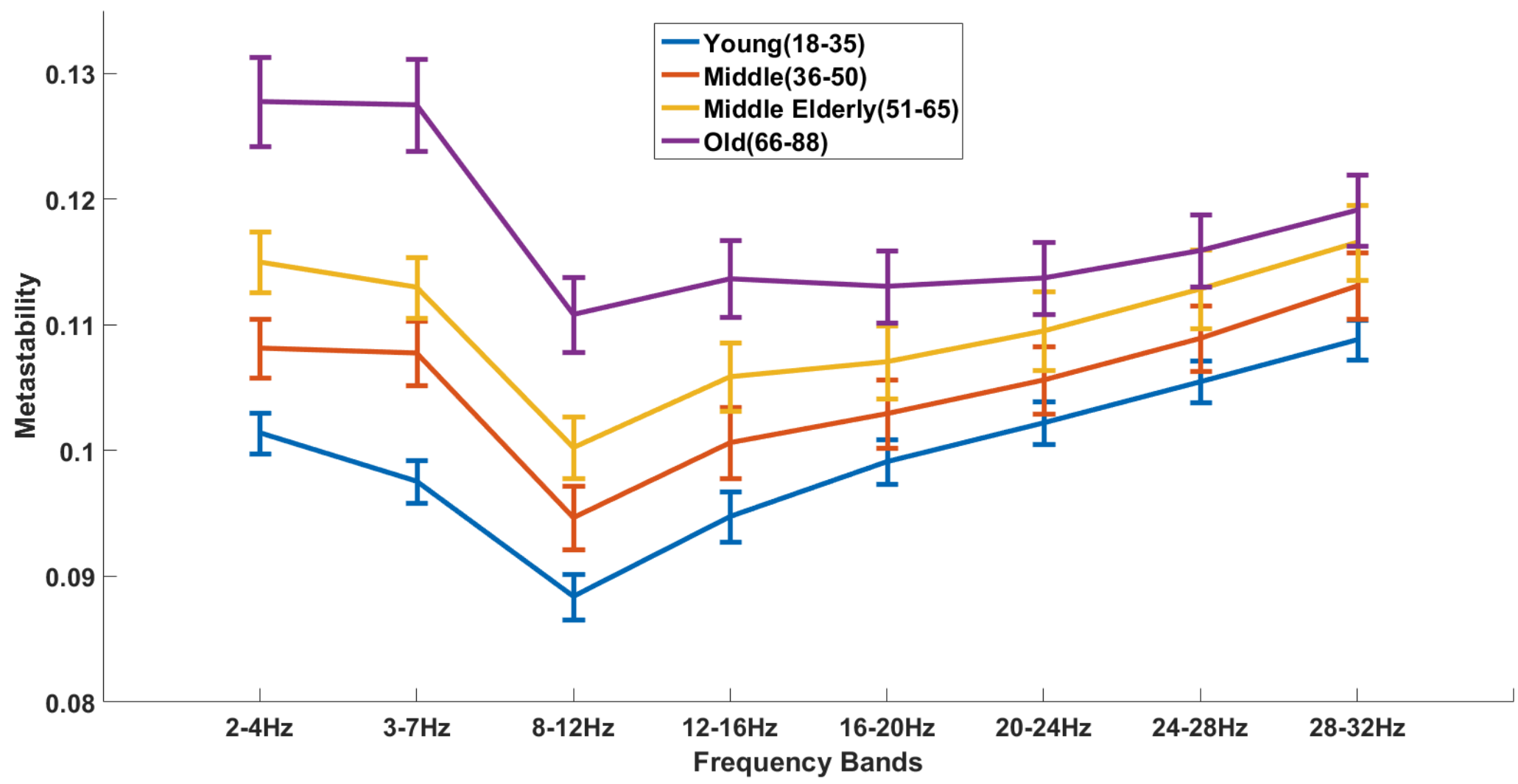

B. Band specific metastability

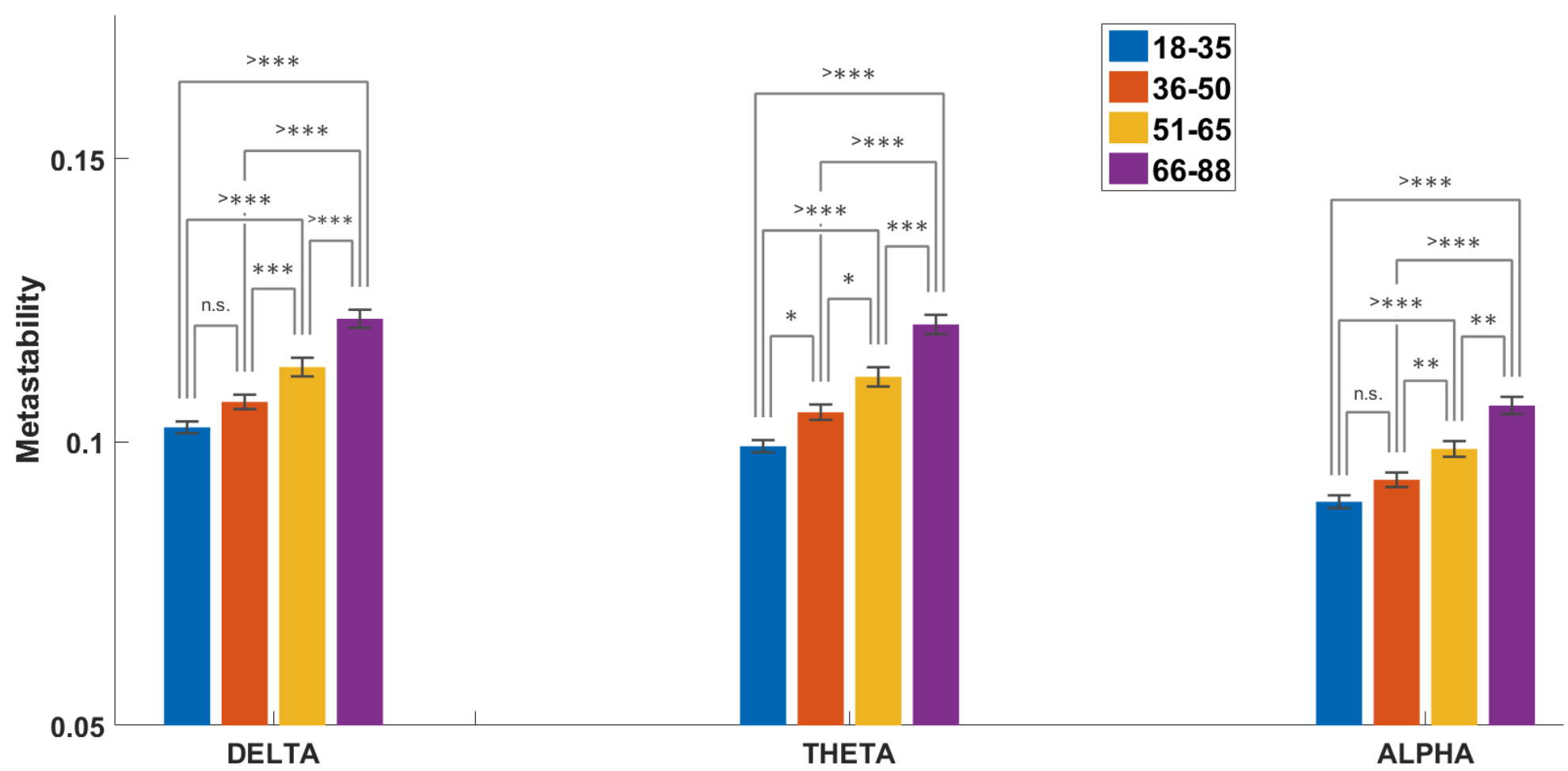

C. Metastability in smaller age groups

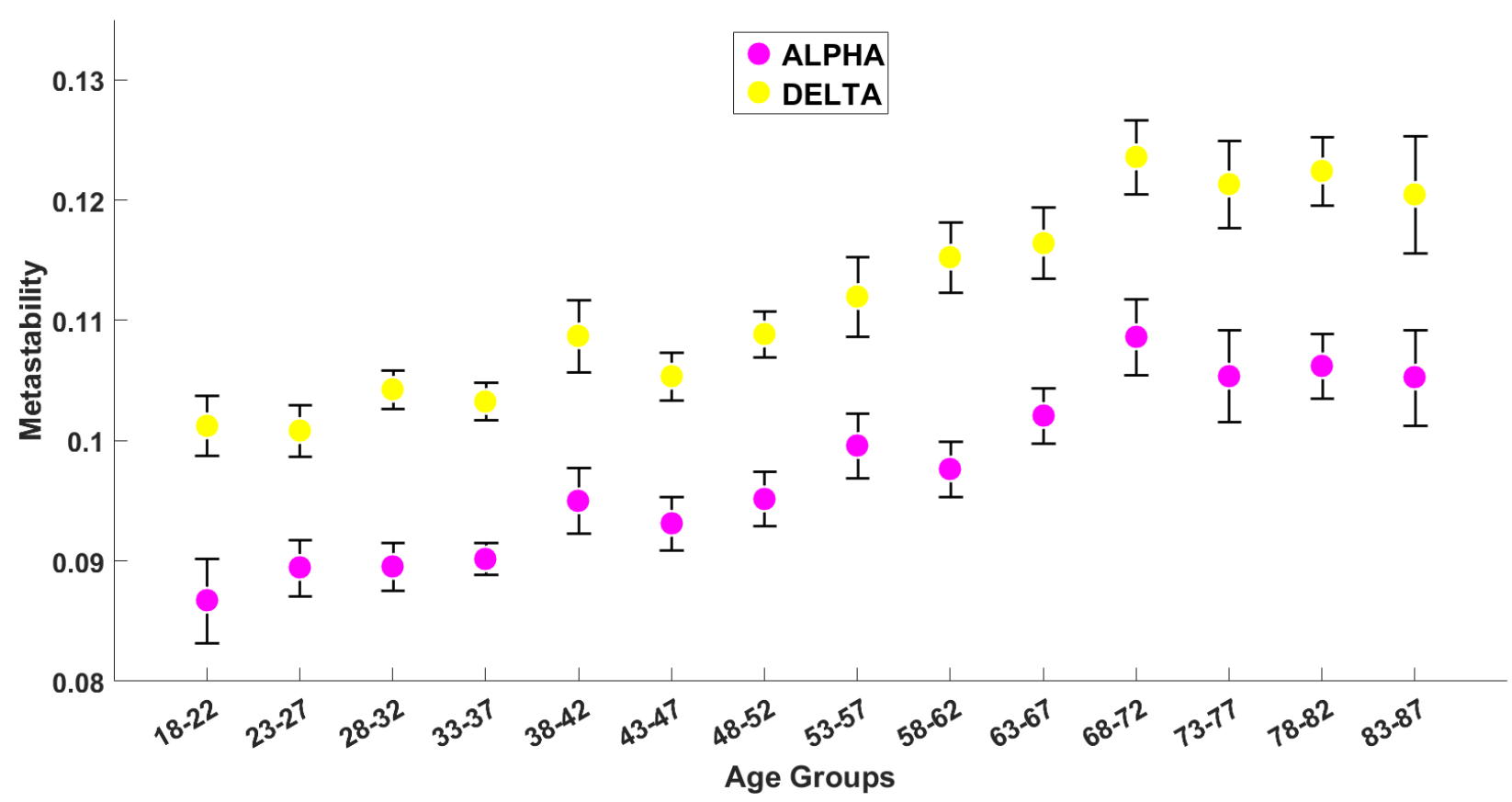

D. Slow and fast time scales of metastability

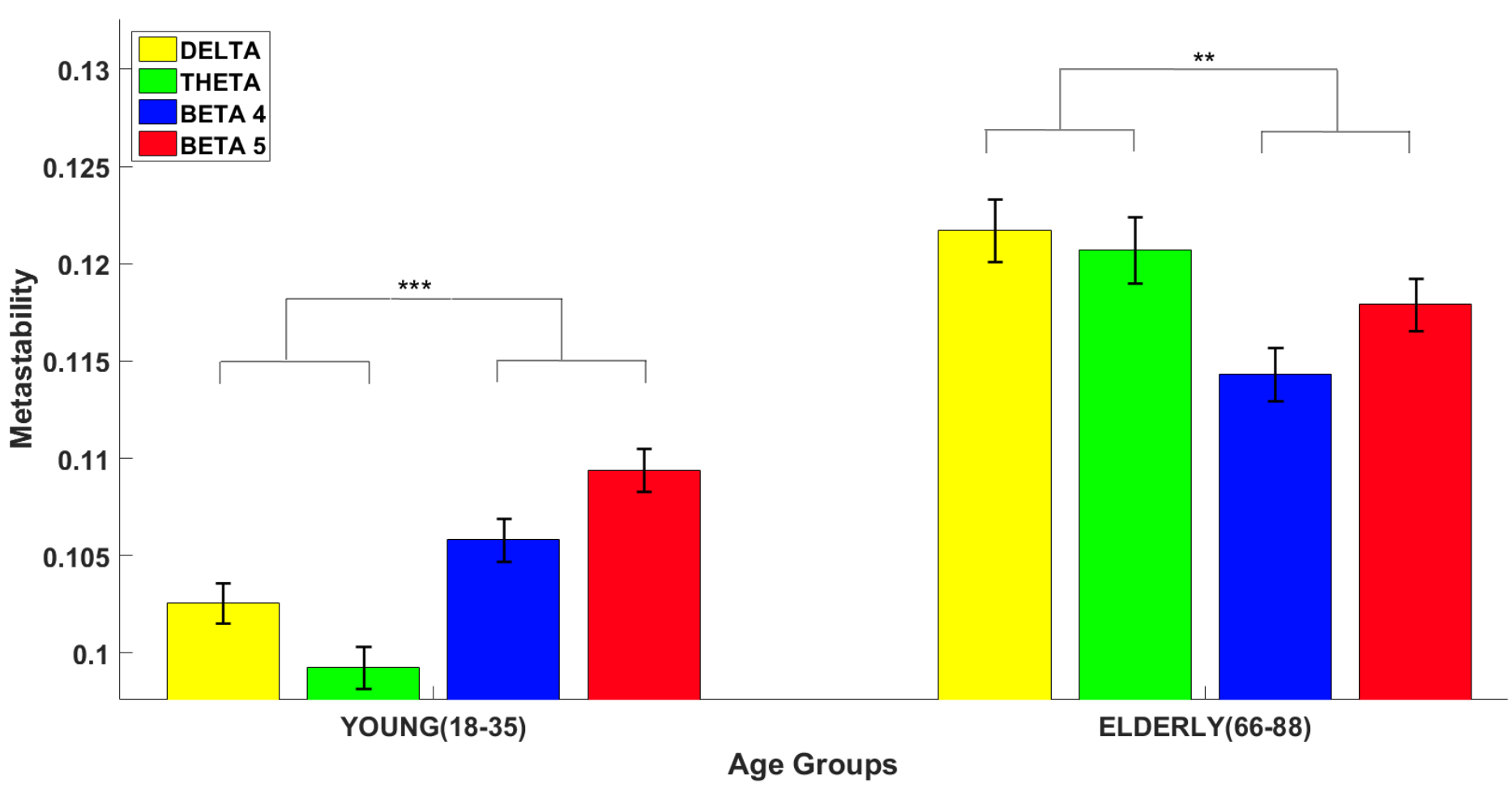

Figure 5.

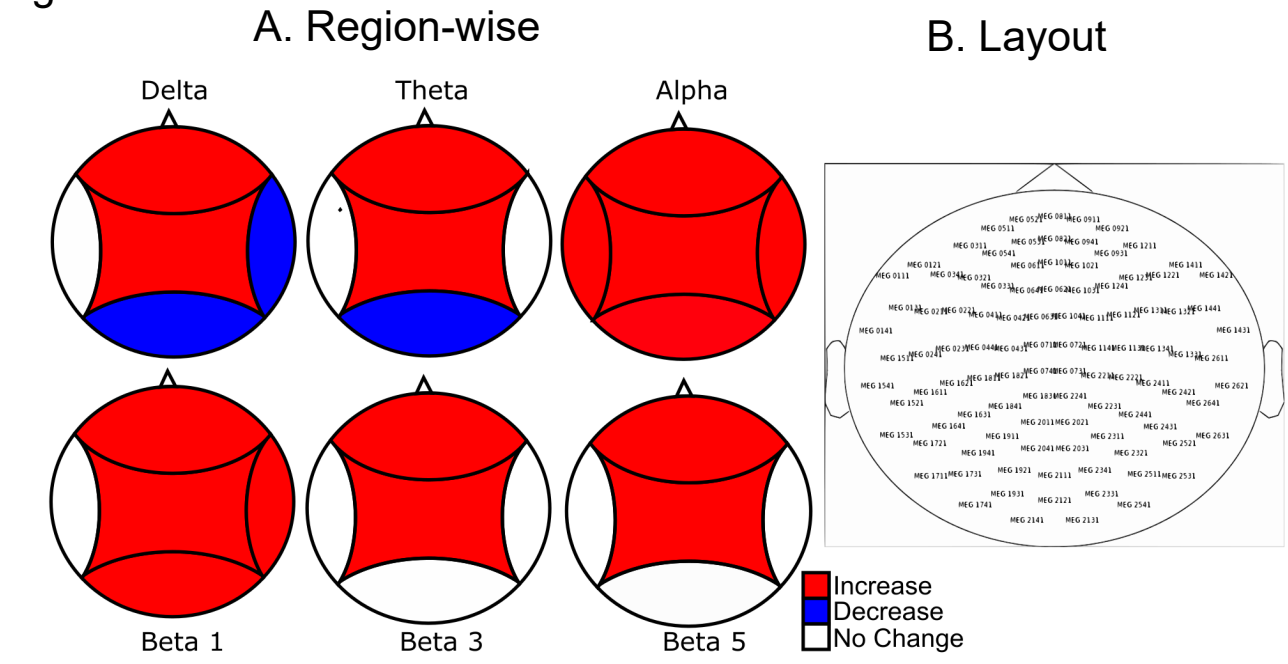
A. Region-wise
B. Layout
Delta
Theta
Alpha
Beta 1
Beta 3
Beta 5
Increase
Decrease
No Change

Figure 6a.

VSTM task precision with age

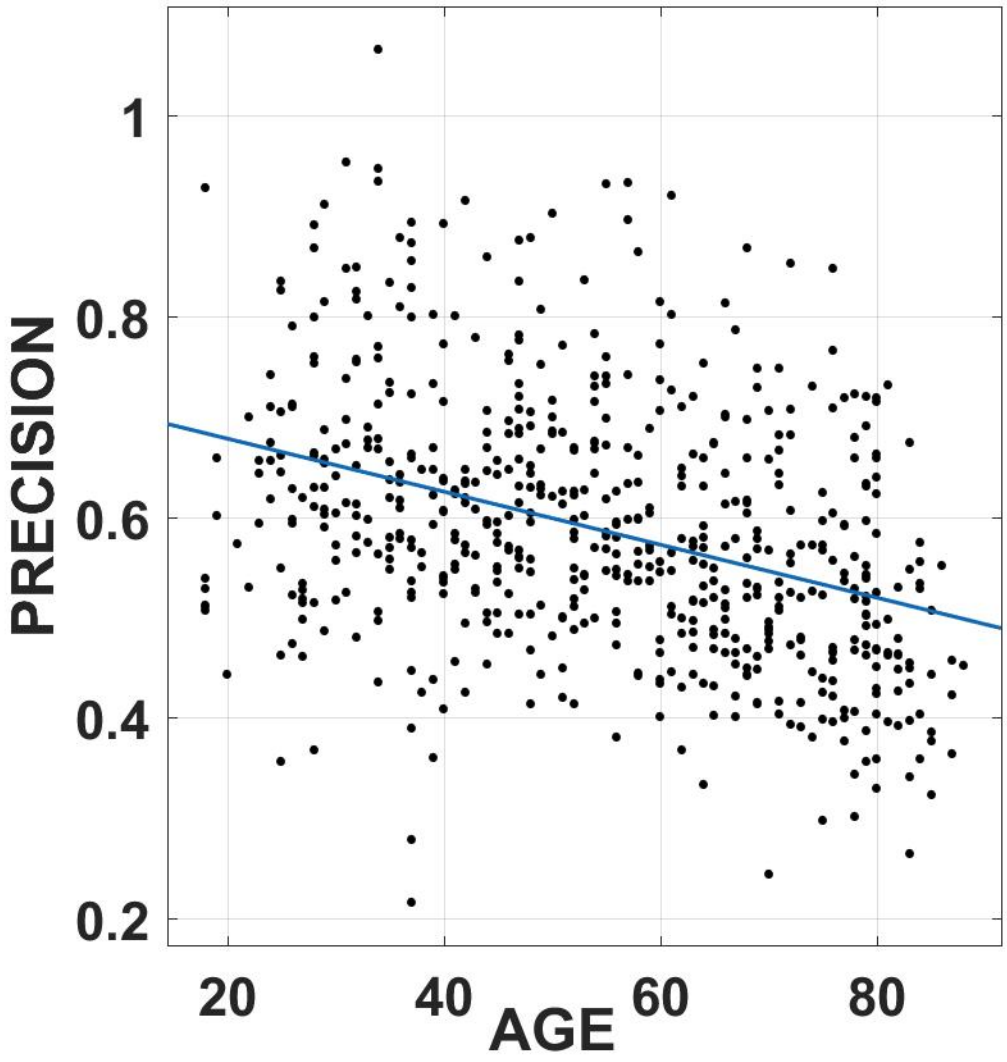

Figure 6b.

Global Coherence(Alpha Band) Vs Precision in VSTM task

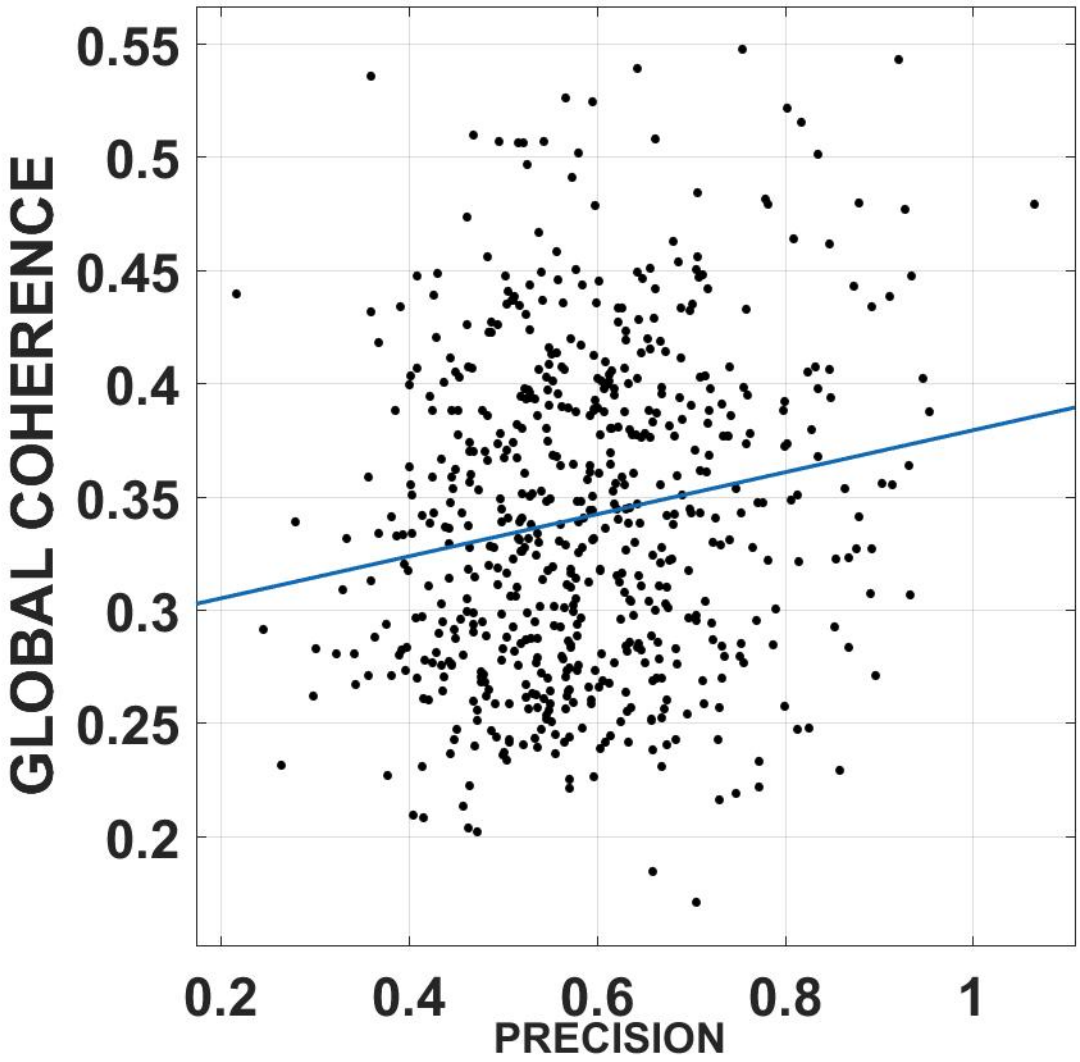

Supplementary fig 1a.

ICA Corrected Delta Band(1-3 Hz) global coherence with age

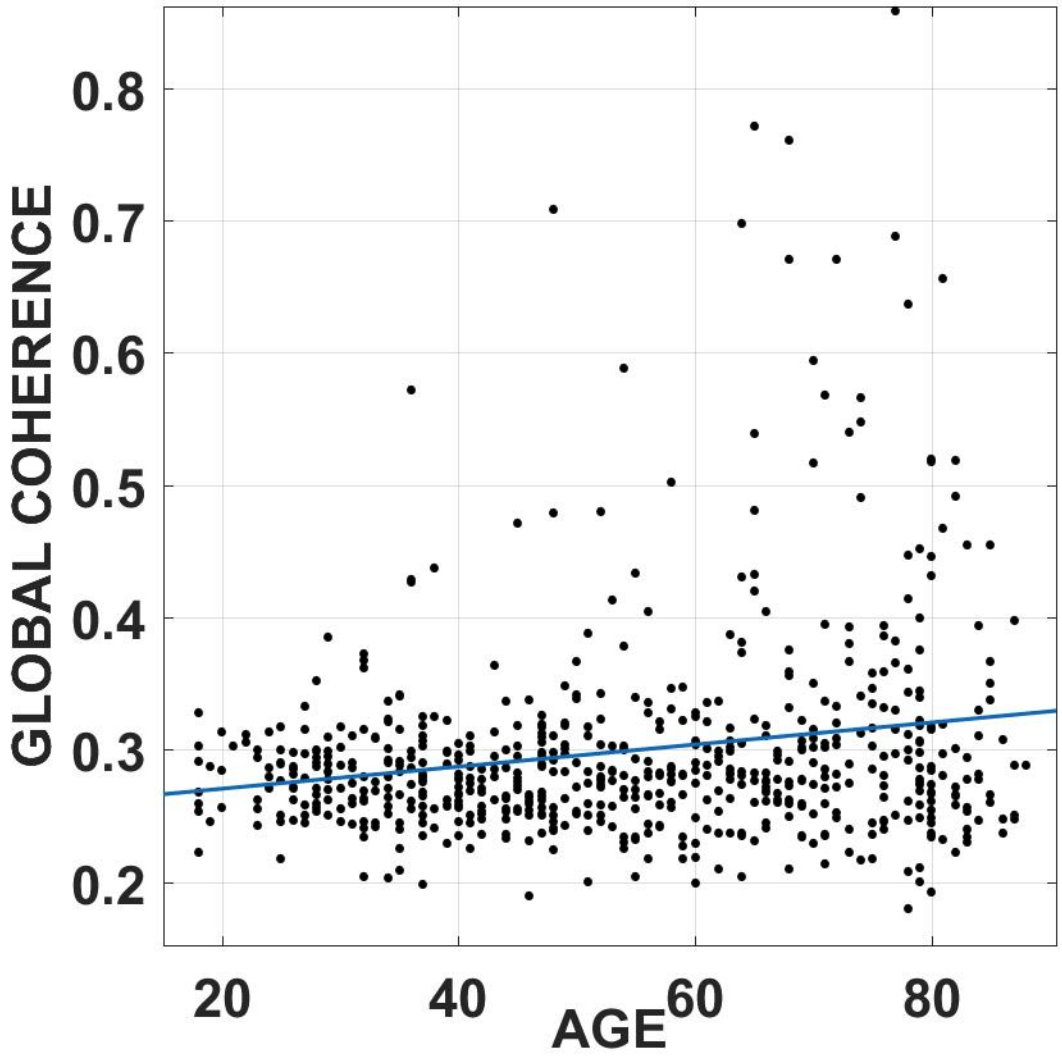

Supplementary fig 1b.

ICA corrected Theta Band(3-7 Hz) global coherence with age

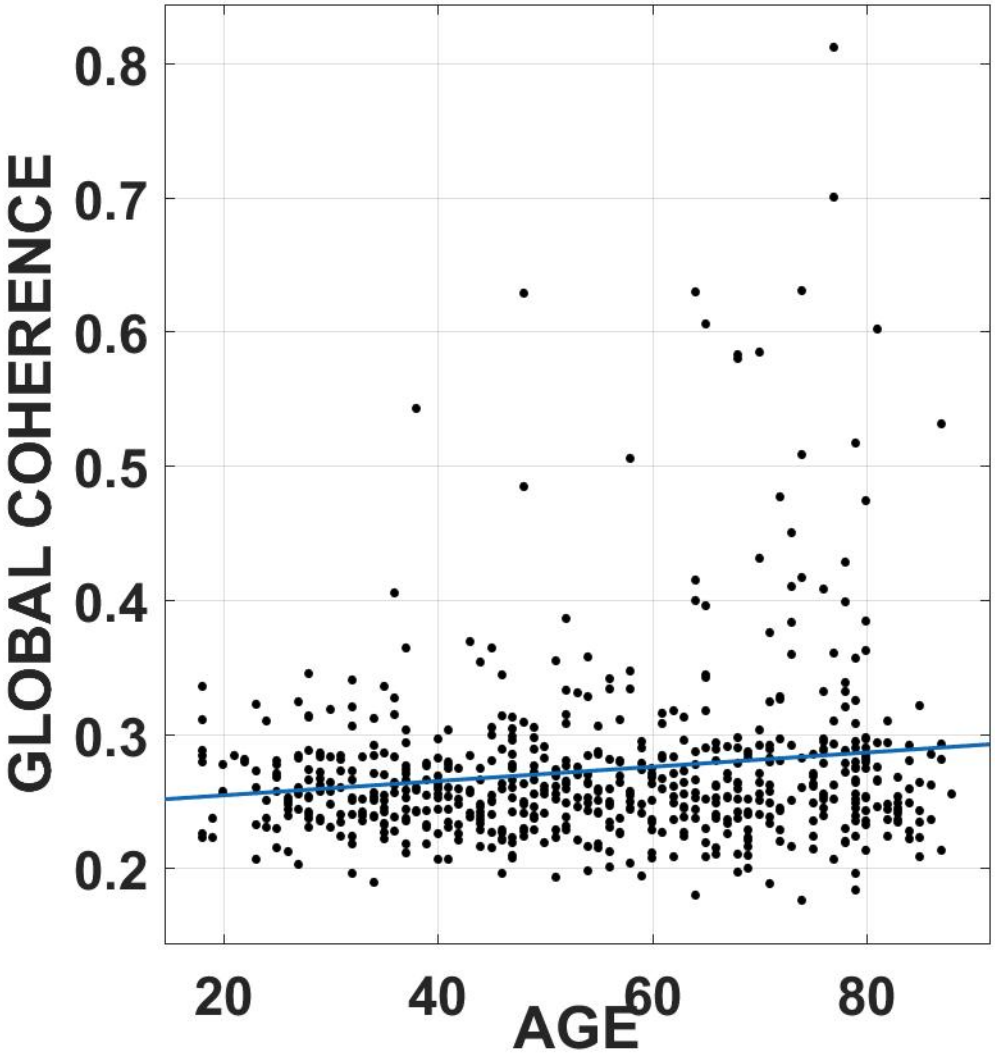

Supplementary fig 1c.

ICA corrected Alpha Band(8-12 Hz) global coherence with age

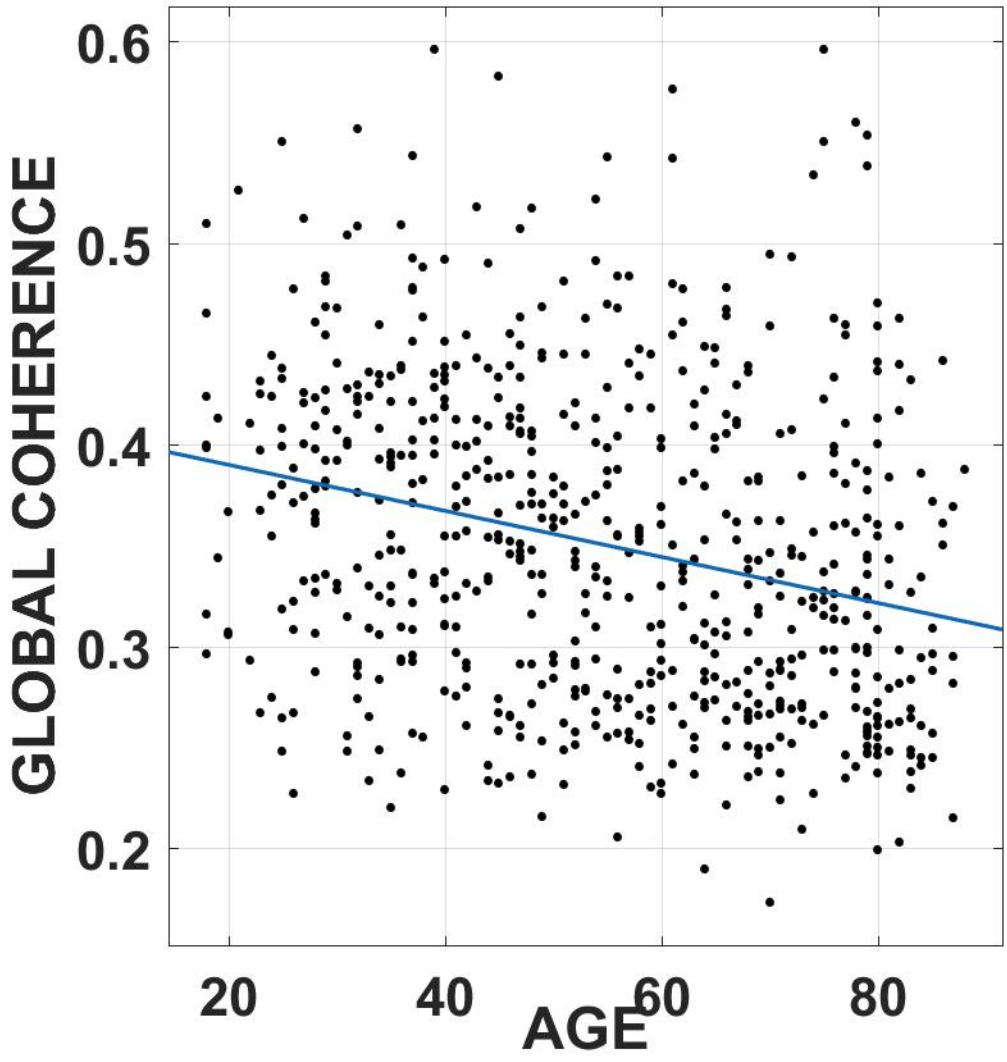

Supplementary fig 1d.

ICA corrected Beta Band(16-25 Hz) global coherence with age

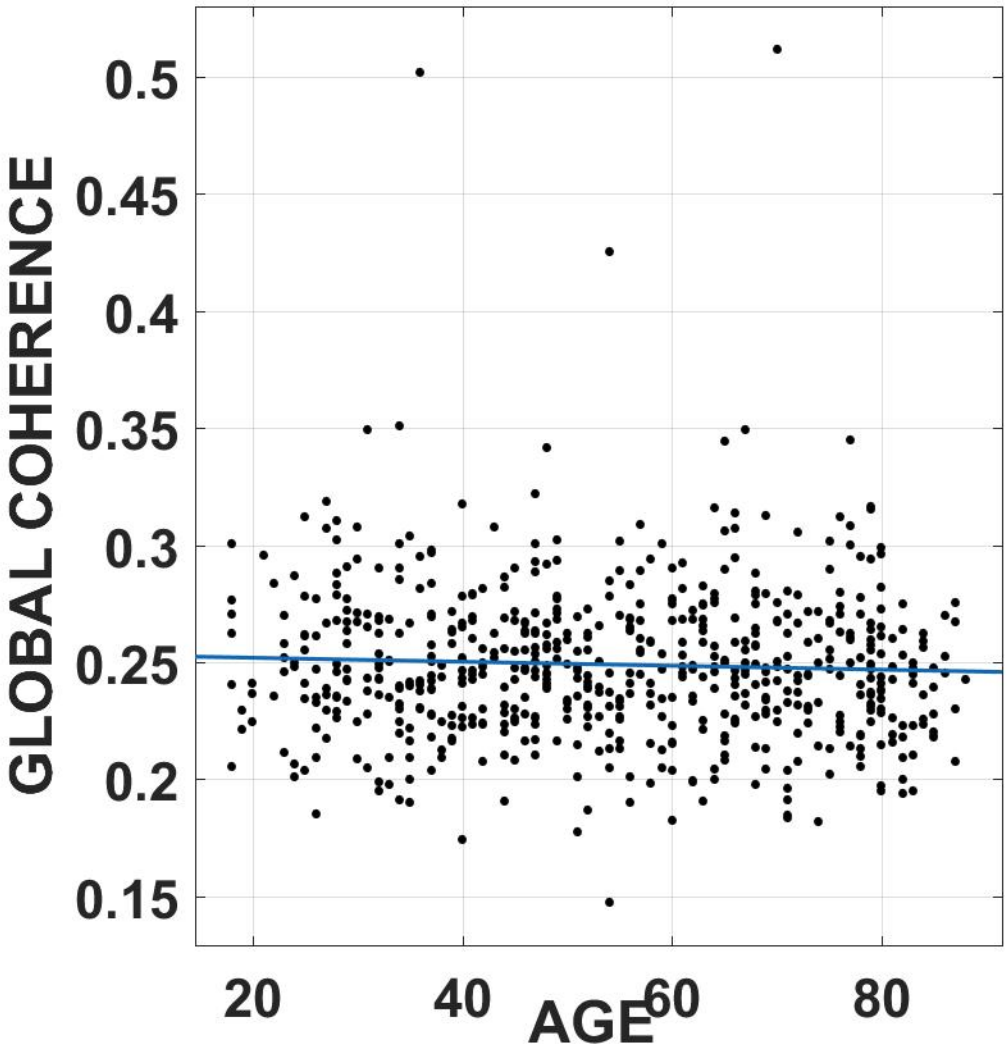

Supplementary fig 1e.

METASTABILITY IN DELTA(2-4Hz) BAND(ICA CORRECTED)

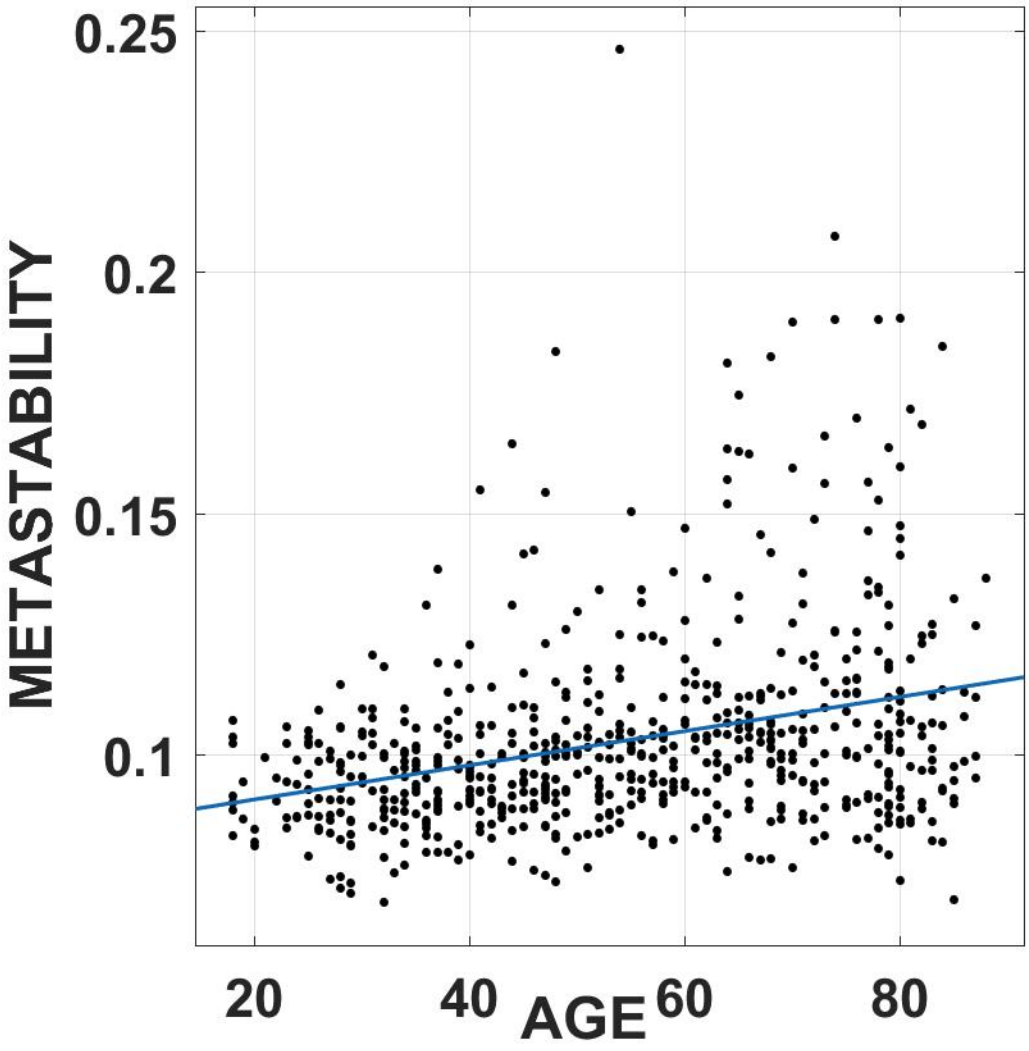

Supplementary fig 1f.

METASTABILITY IN ALPHA(8-12Hz) BAND(ICA CORRECTED)

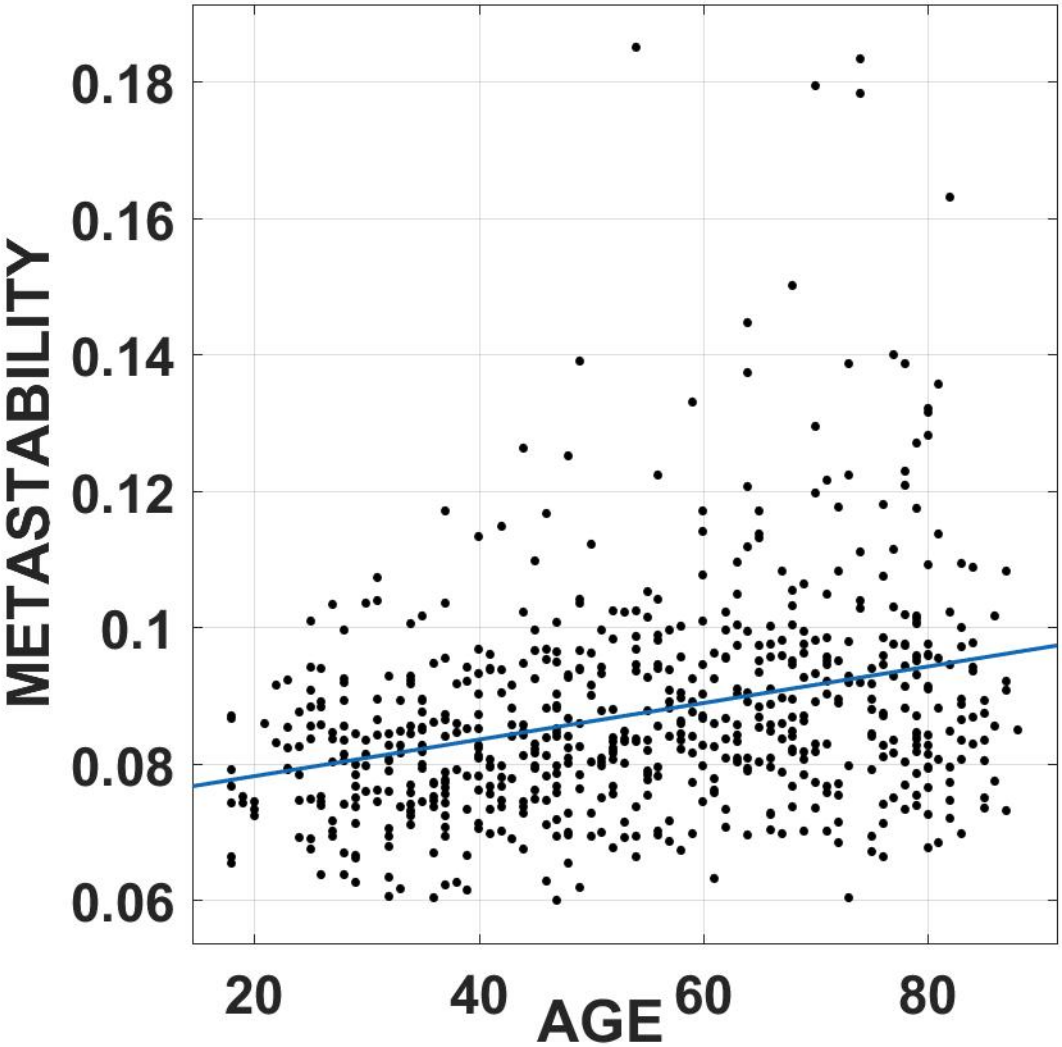

Gender-wise comparison of randomly sampled age groups

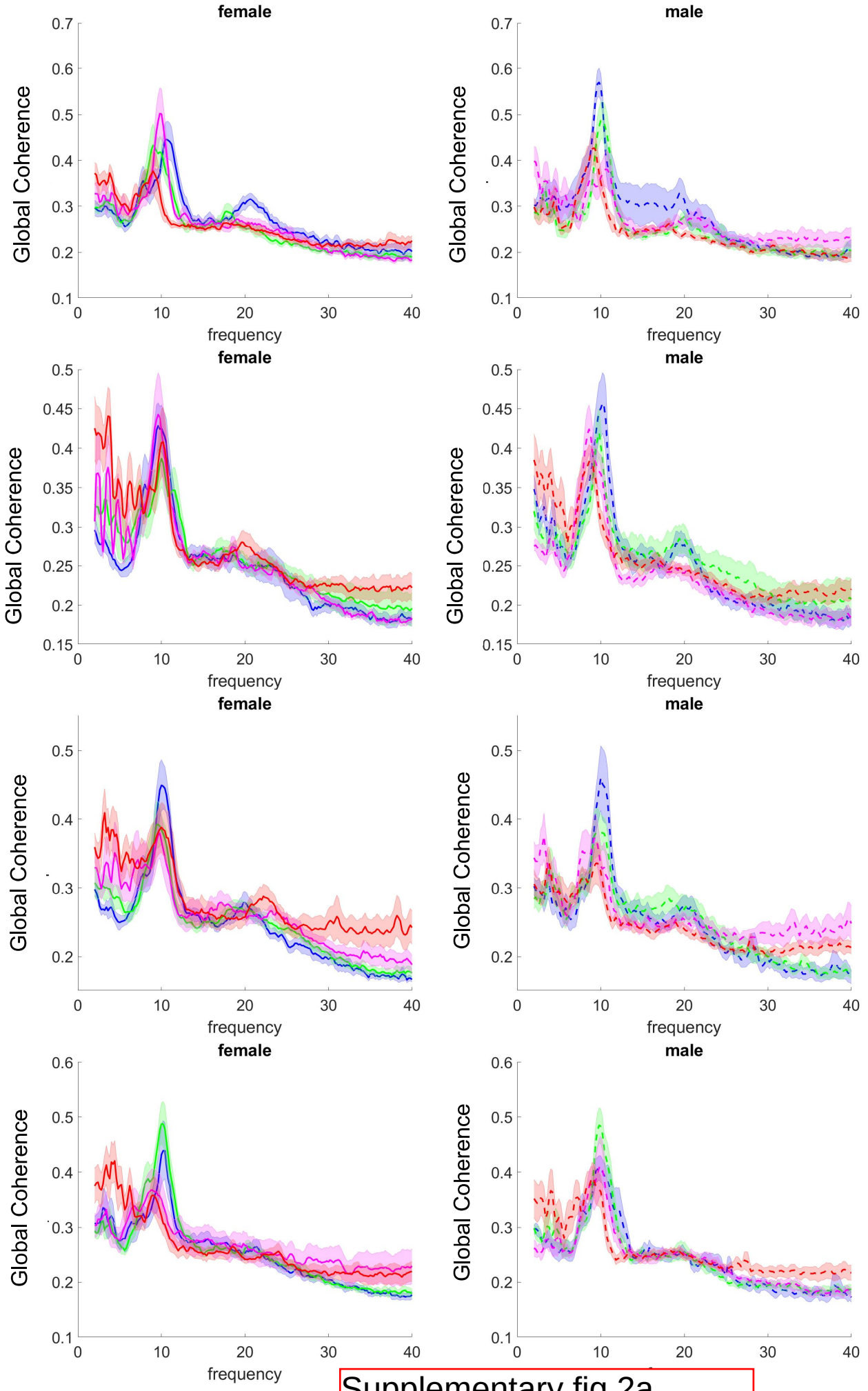

Supplementary fig 2a.

Supplementary fig 2b.
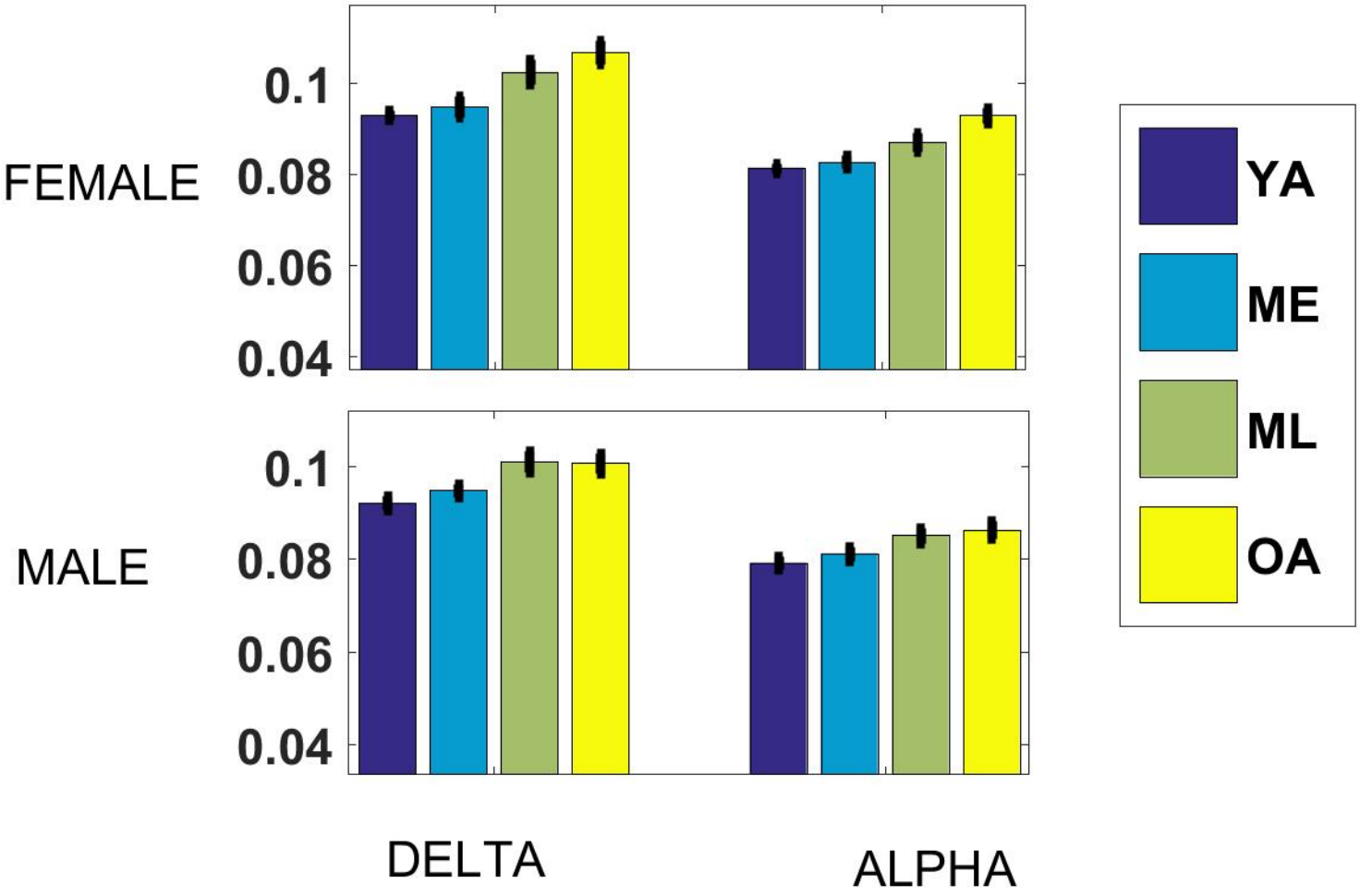
Gender-wise metastability in delta and alpha band